Climate control in broiler houses: a thermal model for the calculation of the energy use and indoor environmental conditions

Andrea Costantino[1], Enrico Fabrizio[1*], Andrea Ghiggini[2], Mauro Bariani[2]

[1]*DENERG, Politecnico di Torino, TEBE Research Group, Corso Duca degli Abruzzi 24, 10129 Torino, Italy*

[2]*Munters Italy S.p.a., via Strada Piani 2, 18027 Chiusavecchia d'Imperia (IM), Italy*

*Corresponding author. Tel: +39 011 090 4465; Fax: +39 011 090 4499
E-mail address: *enrico.fabrizio@polito.it*

Abstract

The use of energy in the livestock sector will rise in the years to come due to the increasing demand for animal proteins from a word population that will reach 9.15 billion people before 2050. Livestock houses for intensive animal farming are characterized by high energy consumption due to climate control that is needed to guarantee animals' welfare and to maximize their production. Currently, there are neither international standards calculation models nor commercial tools for the estimation of this energy consumption. To fill this gap, this paper presents a simulation model (based on a customization of the hourly model of ISO 13790) for the estimation of the energy consumption due to climate control of broiler houses. This model provides the energy consumption for heating, cooling and ventilation and the main indoor environmental parameters for the evaluation of the animals' welfare. The model was validated comparing its outputs with a dataset obtained through a monitoring campaign carried out in a broiler house during a production cycle. This research has several practical application: it can increase the knowledge about energy consumption in the livestock sector and the model can be also a useful tool for agricultural engineers and farmers.

Keywords: climate control, energy consumption in livestock houses, simple hourly method, broiler farming, energy model.

1 Introduction

The use of energy in the livestock sector will play a fundamental role in the near future because the energy needed to meet the demand for animal proteins will rise in the years to come. The world population is expected to increase considerably: according to UN research [1], the number of people that will have to be fed in 2050 will reach 9.15 billion, an increment of about 22% if compared to 2017. This occurrence will entail an increment in animal protein consumption that will become almost twice the current amount [2], considering the diet changes that are expected. In particular, FAO [3] has estimated that in 2050 the consumption of poultry will increase by 230% if compared to 2010, while the consumption of other livestock products will increase by about 40-80% over the same period.

The rise in energy consumption is not the only issue concerning the increase in animal production that may be investigated. Others, for example, are the increase in water consumption, production costs and greenhouse gas emissions [4]-[7]. However, the energy consumption issue becomes even more important if it is considered together with the shift in technology that is expected in the agricultural and livestock sectors in the near future and that will further increase the energy needs in these fields [8]. Considering that the price of non-renewable energy sources is predicted to rise, the energy topic in the livestock sector becomes crucial. For this reason, knowledge about energy performance and energy use in all the branches of this field is fundamental to achieve a considerable energy saving and a higher level of sustainability.

Livestock houses for intensive animal farming are of particular interest because they could offer many opportunities for increasing energy performance. These buildings, in fact, are generally characterized by high energy consumption for different uses and, depending on the reared species, climate control can represent a considerable share of the total energy consumption of the breeding farm. In dairy cow farming, the energy used for climate control is 27.4% of the total electrical energy, an amount almost equal to the energy needed for milking tasks (28.3%) [9]. The energy needed for climate control is higher in pig farming due to the different climate requirements of swine. In fact, pigs, and especially piglets, need to be kept warm during the coldest periods of the year. In Europe, this need entails an estimated energy consumption between 34 and 37 $kWh \cdot m^{-2} \cdot a^{-1}$ of electrical energy to provide adequate local heating and ventilation to the animals [10], which corresponds to 48% of the total electrical energy needed during the entire rearing process [9]. Poultry houses also need a great amount of energy for climate control. Laying hen farming uses between 15 and 20 $kWh \cdot m^{-2} \cdot a^{-1}$ for ventilation (58.9% of the total electrical energy needed), while in broiler (chicken reared for meat) farming almost all the energy is used for climate control (76% of the total electrical energy and 96% of the total thermal energy). In detail, it was estimated that a typical European broiler house consumes between 86 and 137 $kWh \cdot m^{-2} \cdot a^{-1}$ for heating and between 4 and 11 $kWh \cdot m^{-2} \cdot a^{-1}$ for ventilation [9] [10]. Different weather conditions, different features of the animal farming (e.g. stocking density) and different building characteristics (e.g. internal volume and U-values of the envelope) may modify these values.

Indoor climate control entails a considerable energy consumption but its presence is fundamental in livestock houses because it strongly influences the health, growth and the performance (e.g. production of eggs or milk) of the animals and, consequently, it affects the farm profits. To have an acceptable level of productivity, the effective environmental temperature inside the livestock houses has to be considered. This temperature takes into account various environmental parameters, such as dry bulb temperature, wet bulb temperature and air velocity and it should be in the zone of nominal losses [11], a thermal neutral temperature range between the Lower Critical Temperature (LCT) and the Upper Critical Temperature (UCT). In the zone of nominal losses, the energy fraction used by animals for maintaining their homeothermy is at a minimum, therefore the animal can use most of the energy supplied by feed for its growth and/or for the production of milk or eggs. Values of effective environmental temperature higher than the UCT for extended periods may lead the animal to suffer from hyperthermia, therefore the animal stops feeding. Temperature values lower than the LCT, on the contrary, may cause hypothermia. In this situation, the animal uses the energy from its feed to increase its metabolism and, consequently, its body temperature. Therefore, when the effective environmental temperature is outside the zone of nominal losses, the health and the productivity of the animals are not at the optimal level, causing negative consequences for the farm profit.

To guarantee an adequate indoor environment, it is necessary to intervene on air temperature, moisture and Indoor Air Quality (IAQ). Temperature control is crucial for some animal species, especially in the first period of their lives because they are very sensitive to temperature variations (e.g. chicks and piglets). For other animal species, temperature control is not fundamental because the range between LCT and UCT is larger (e.g. dairy cows and sheep), thus the animal houses for these species can be operated in free running conditions during most of the time. Moisture has to be controlled because high values of relative humidity (RH) may increase the thermal stress of animals and cause health problems. Finally, IAQ control plays a more important role in livestock houses than in other building types because many contaminants present in these buildings are biologically active (due to airborne microorganisms), their concentration is extremely high if compared to other buildings and they are odor carriers [12].

The principles for climate control in livestock houses are similar to those of buildings destined for human use, but the peculiarity of the indoor conditions makes the climate control in these houses even more interesting from an engineering point of view. In broiler houses, for example, the high animal stocking density entails a sensible heat emission estimated approximately in 180 $W \cdot m^{-2}$ and a vapor emission of 5.2 $kg_{vapour} \cdot m^{-2} \cdot day^{-1}$ during the last days of the production cycle. Furthermore, in this building type, the indoor climate conditions that have to be guaranteed depend on the animal breed and age and on the adopted type of animal farming. For example, it is common for a broiler house to need a heat load in summer periods too, due to the presence of chicks.

In this scenario, a model for the estimation of energy consumption due to climate control and indoor conditions (e.g. indoor air temperature and RH) is of the foremost importance. Currently, there are neither international standards calculation models nor commercial tools that make possible to estimate these data, considering the performance of both envelope and systems. Such a model would be interesting for both agricultural engineers and farmers because it could help the former in the design stage and the latter during the management stage. In fact, through such a model the evaluation of energy saving strategies (e.g. retrofitting actions and use of new commercial products) and a better planning of the production process (e.g. production costs related to weather conditions) may be possible.

1.1 Aim of the work

The aim of this work is the development of a calculation model that allows the estimation of the energy consumption for climate control (heating, cooling and ventilation) and the indoor environmental parameters (air temperature and RH) in broiler houses for intensive animal farming.

Broiler farming was chosen for the development of this calculation model because it has the highest share of energy consumption due to climate control in the animal farming. From an engineering point of view, broiler rearing is relevant since it is carried out in a totally closed enclosure, which simplifies the estimation of the ventilation flow rate. Furthermore, there are specific conditions that are uncommon in buildings for human use, such as the variable set point temperatures and the considerable internal loads. Moreover, broilers represent the second meat market worldwide (96.1 million tons produced in 2013) [13], therefore it considerably influences energy consumption of the livestock sector.

To predict the energy consumption of climate control systems used in livestock houses, dynamic simulation models are needed because they make it possible to take into account the strategies of passive climate control and the sudden variation of the boundary conditions [14]. In this sector, self-made and customized calculation models are usually preferred to ready-to-use simulation models (e.g. TRNSYS and EnergyPlus), as shown in literature [15]-[17]. This is due to the difficulty of ready-to-use models to accurately define the thermal behavior of livestock houses and the boundary conditions. Furthermore, the level of customizability of self-made models is high and, for this reason, they proved to be more adaptable to the specific objectives of the present work.

The developed simulation model is based on a customization of the simple hourly method described in the ISO 13790 Standard [18] that is based on a similarity between the thermal behavior of the considered building and a 5R1C (five resistances and one capacitor) electric equivalent network [19]. The reliability of this calculation method has been proved by a number of previous studies [20]-[25] and it is considered accurate in describing the thermal behavior of livestock buildings [26]. The adopted time step of the method (one hour) is sufficiently short to correctly consider the variations of the outdoor and indoor conditions without weighing the calculation down with excessive iterations. The disadvantages with respect to ready-to-use models lie in the fact that customized models generally do not extensively analyze the total thermal capacity of the building, the solar radiation calculations and do not explicitly solve the radiation exchanges within the enclosure.

The presented model gives as outputs the values of the energy need for heating and ventilation expressed as total value, a value referred to the unit of useful floor area and a value referred to the kg of produced meat. Inputting the cost of energy, the annual costs due to climate control can be obtained. The model also provides some environmental parameters, specifically indoor air temperature and RH, which is useful for the calculation of environmental indexes for evaluating the thermal conditions of the animals during the analyzed period [27].

2 Broiler farming

2.1 Broiler rearing

Broiler houses are quite standardized buildings. They usually have a maximum width between 10 and 15 m and a length that may exceed 100 m. The covering can be a gable roof or a barrel vault that in the highest point reaches 4 or 5 m of height [28]. The windows and the opening systems that are present in this building type depend on the ventilation scheme [29], but generally they are made of polycarbonate hollow sheets adopting a guillotine or wasistas opening system. The U-values of the envelope are usually higher than the ones that are present in residential buildings, since, commonly, perimeter walls and roof have only few centimeters of thermal insulation layer.

The production cycle carried out in a broiler house is called batch. It starts when few-days-aged chicks are carried inside the building where they will stay during 40-50 days, until they achieve the target weight for being slaughtered. At the end of the batch, the workers handle the sanitization of the house. This sanitary empty period could take between 7 and 14 days to be carried out. Considering these production breaks due to sanitary needs, about 7-8 batches can be completed during a year. The animal stocking density in intensive broiler rearing typically goes from 33 to 42 $kg \cdot m^{-2}$ of live weight (as set by European Council Directive 2007/43/C [30]) that approximately corresponds to a value between 9 and 22 $birds \cdot m^{-2}$ [31], depending on the aimed final live weight that generally is about 2-3.5 kg. The final live weight of the animal does not correspond to the chicken meat that may be sold on the market: for obtaining this value, a carcass yield (the ratio between the saleable meat obtained from the animal and its final live weight) around 73% has to be considered [32].

2.2 Climate control in broiler houses

From the point of view of the climate control, changes that occur in broiler houses during a batch appear interesting. The first part of the batch is characterized by the presence of few-days-aged chicks that need high air temperatures in order to be in a state of thermal comfort. Therefore, during the first days of batch the system heats the enclosure. The air temperature needed for guaranteeing the health of the broilers decreases inversely with the animal age, therefore, during the rest of the batch, the indoor air temperature set point decreases due to the bird growth and cooling is needed [16]. The presence of older and heavier birds inside the house during the central and last parts of the batch entails a higher ventilation flow rate that is required to remove their body thermal emissions and the higher concentration of contaminants produced.

Heat and vapor emissions of a broiler change significantly during the batch. On the first day of the production cycle, a total heat emission of about 1.3 W can be considered for a single chick and this value increases until 26 W at the end of the batch (50^{th} day). Similarly, vapor emission of a single animal can be estimated as $3 \cdot 10^{-7}$ $kg \cdot s^{-1}$ (at an indoor air temperature of 32.0 °C) when the batch starts, while at the end of it this value reaches $4.5 \cdot 10^{-6}$ $kg \cdot s^{-1}$ (at 16.8 °C) [33]-[35]. Those data (e.g. heat emissions and indoor air set point temperatures) are necessary to set correctly the mechanical climate control systems. Usually, in broiler houses, a heating system (generally gas air heater or diesel air heater) and one or more ventilation systems are present. Air heaters are activated during the first period of the batch to guarantee high indoor air temperature set points needed by the chicks, while ventilation has a double purpose. In fact, two different types of ventilation systems are present: base and tunnel ventilation. Base ventilation (Fig. 1) is required for controlling IAQ in the house. Air composition in a closed environment where animals are hosted is influenced by a number of factors. First, by animal metabolism that consumes oxygen and increases the concentrations of CO_2 and vapor (a not adequate moisture level can cause respiratory problems to birds); second, IAQ is conditioned by animal activities and air movements that contribute to increase the presence of contaminants in form of microscopic particles of dust originated from bedding, feed and fecal material [36]. The decomposition of waste products influences IAQ too, since methane, hydrogen, sulfide and ammonia are produced; in particular, ammonia (present in broiler manure) is responsible for eyes or paws irritations and is the cause of other health problems for broilers. Furthermore, high ammonia concentration can affect the health of the workers present inside the broiler house. For these reasons, farmers usually adopt strategies for reducing the ammonia emissions from the houses [37].

Base ventilation is useful for IAQ control, especially for gas concentration regulation (e.g. methane and vapor), but it may not be sufficient for dust control because pockets with high contaminant concentrations are common in animal houses and different strategies (e.g. spraying and sprinkling) should be adopted to control dust concentration [12] [38]. To provide base ventilation, several fans are spaced uniformly along one of the larger sides of the house and on the opposite side or on the roof ridge various openings are present, with different inlet configurations [28].

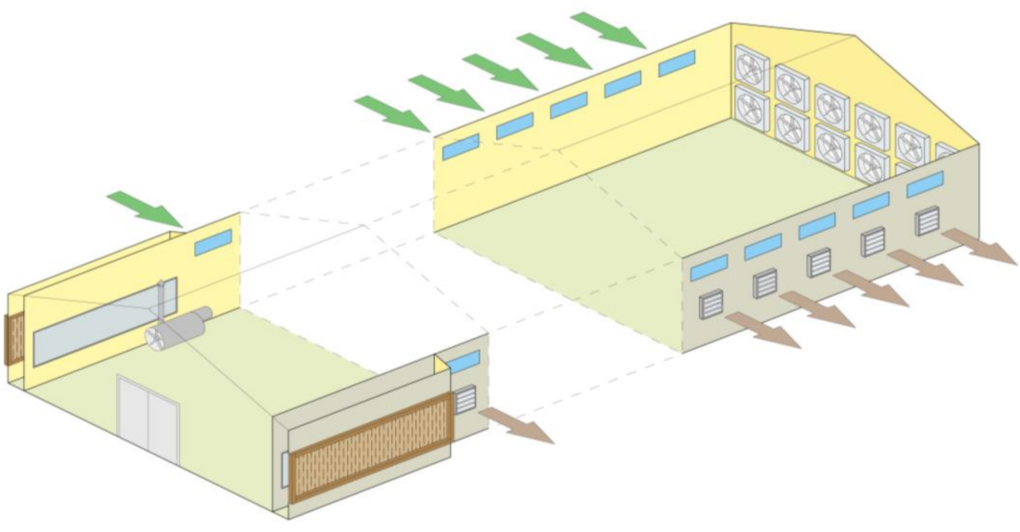

Fig. 1. Illustration of base ventilation operating principle. Lateral fans create a negative pressure inside the house expelling the exhaust air (brown arrows) outside. Supply clean air (green arrows) enters through the windows on the opposite wall, creating a ventilation flow in the cross direction that guarantees IAQ control.

Due to the location of the fans and the openings, base ventilation flow rate occurs following the cross direction [36]. Base ventilation may be a positive-pressure or negative-pressure ventilation, depending on the scheme adopted in the house.

The second type of ventilation adopted in broiler houses is tunnel ventilation (Fig. 2) and is so called because fans (situated in one of the two shorter sides of the building) move the air horizontally along the entire length of the house. Tunnel ventilation fans have greater dimensions than the ones used for base ventilation and are generally exhaust fans that work creating a negative pressure in the animal house, letting the external air to enter inside the house. This type of ventilation is intended to decrease the air temperature removing the thermal emission of the animals and providing them wind-chill effect. The air speed of tunnel ventilation in the animal areas cannot be excessive (2.5-3 $m \cdot s^{-1}$ as maximum for poultry in European countries), otherwise animals will be in discomfort.

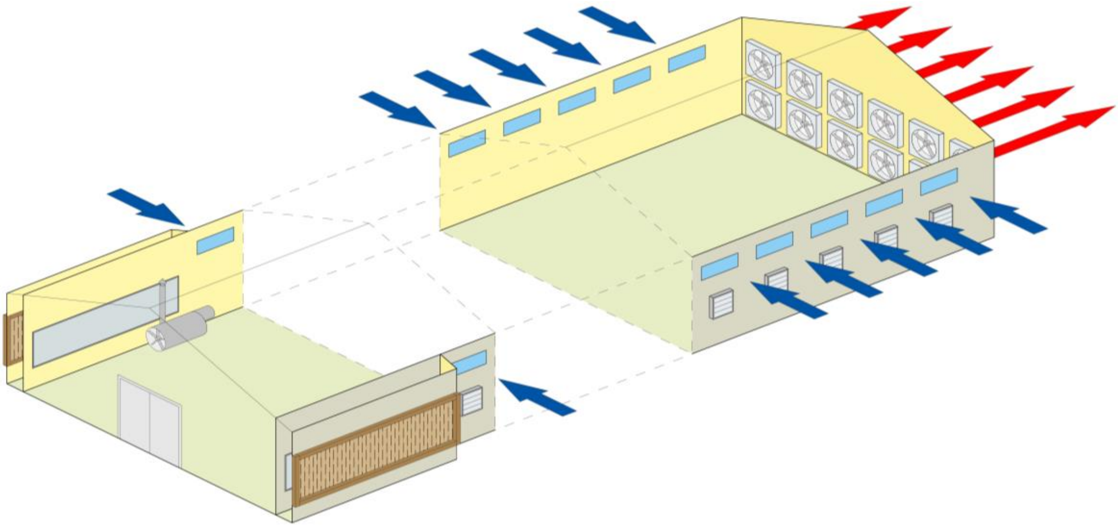

Fig. 2. Illustration of tunnel ventilation operating principle. The fans placed at the end of the house expel hot air (red arrows) outside, creating a negative pressure inside the building. Due to the pressure differential, fresh outdoor air (blue arrows) enters through the inlets placed across the longest sides of the broiler house decreasing the indoor air temperature.

In some broiler houses, the same fans carry out both tunnel and base ventilation. In those houses the smaller fans in the larger sides (the ones used for IAQ control) are not present. The constant flow rate fans at the bottom of the house perform both tunnel and base ventilation. These fans work sequentially because a fan start working when the previous one cannot provide the needed airflow.

When tunnel ventilation is not enough for guaranteeing the indoor air temperature set point, evaporative cooling is activated. This strategy is commonly used in poultry houses (Fig. 3) and can provide a supplementary cooling load to prevent heat prostration mortality during the warmest periods [36]. This process is based on a conversion of the sensible heat to latent heat carried out by evaporative pads. During the warmest periods, external air passes through the pads due to the negative pressure created by tunnel ventilation fans. This process decreases the inlet outdoor air temperature of some degrees and, consequently, the indoor air temperature decreases. Evaporative cooling is more effective the lower the outdoor air humidity is.

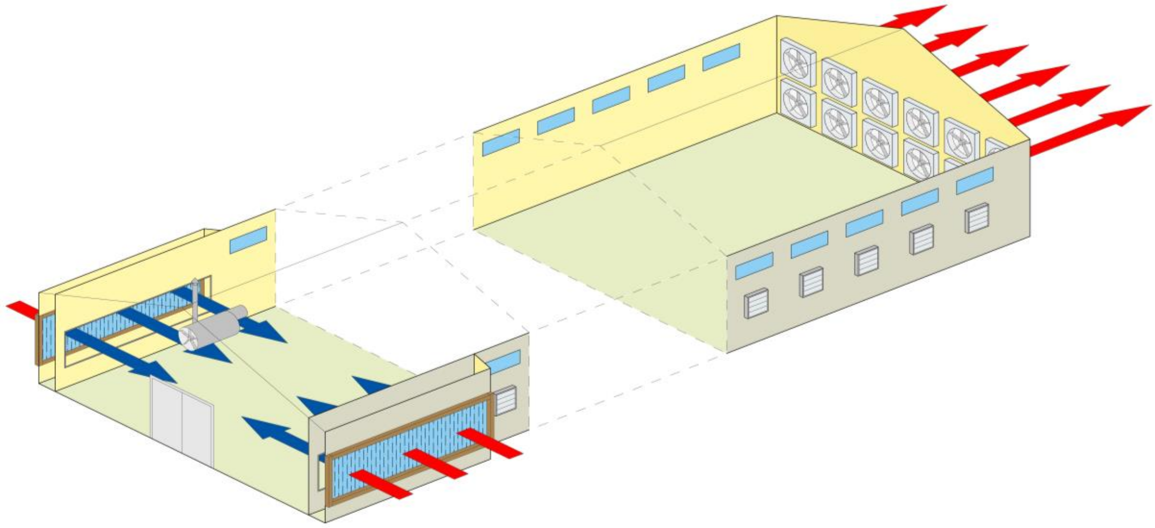

Fig. 3. Illustration of evaporative cooling operating principle. The negative pressure inside the house created by tunnel ventilation fans lets the hot external air pass through the wet evaporative pads decreasing its temperature (red/blue arrows). This air decreases the indoor air temperature and is expelled by the tunnel ventilation fans (red arrows).

In broiler houses, cooling pads are placed on the larger sides opposite to the tunnel ventilation fans for letting the cooled airflow cross the entire building. For this application, blocks of corrugated materials as plastic, fiberglass or cellulose (as shown in Fig. 4) are used. Generally, they are treated to absorb more water, increasing their efficiency. Little information are present concerning water demand and usage of evaporative pads since it depends on the pad thickness and the climate conditions: in literature a value of about 12.2 $l \cdot h^{-1}$ per unit of pad area is estimated as average [39].

Fig. 4. Example of cellulose evaporative pads typically used in broiler houses.

3 Modelling of the broiler house

3.1 Background

Works concerning intensive animal farming and use of energy are present in literature. In particular, they regard innovative uses of renewable energy [40]-[42] and the analysis or the monitoring of the main energy consumption in animal houses [43]-[48].

In literature are also present customized calculation models that are commonly used for analyses and studies in the animal farming sector with the final aim of the prediction and investigation of various aspects not only concerning energy consumption, but also to energy ratio index in feed conversion [49], animal growth and mortality [50]-[52] and greenhouse gas emissions [53]. A common application of these simulation models is the forecasting of ammonia emissions from livestock buildings, especially in swine breeding. Measurements of ammonia concentrations are very expensive due to the specialized equipment required [49] [54] and the great number of environmental measurements that are needed for a correct monitoring entails a not negligible financial cost for the farmers [55]. Using simplified but reliable models, the number of needed measurements is minimized as the total cost of the ammonia monitoring.

Computational Fluid Dynamics (CFD) is also adopted to investigate the ammonia emissions in livestock buildings [56], and it is also used for analyzing the airflow distribution in mechanical ventilated animal houses [57] [58]. CFD is used for developing customized models that deal with the homogeneity of air temperature and humidity gradients inside the animal houses, considering the heat and vapor emission of air heaters and animals, and taking into account also the presence of natural ventilation [59]-[61]. Similar models also exist for pig houses [62], aimed to understand how to increase the thermal uniformity in pig breeding. CFD models are also used for studying the convective heat transfer coefficient for a model of a chicken [63].

ASABE Standards (American Society of Agricultural and Biological Engineers) treats various similar issues especially concerning the design stage, such as the design of ventilation systems in poultry and livestock houses [64] [65], the design of lighting systems [66] and the computing of electrical demand [67]. The ANSI/ASABE S612 [68] Standard deals with the performing of the energy audit in farm buildings with the final aim to estimate the energy savings obtainable from the adoption of alternatives in feeding, housing and processing farm animals, but a calculation methodologies for the estimation of the energy consumption for climate control is not provided.

3.2 Model structure

The calculation model presented in this work can estimate the energy consumption values for climate control (heating, cooling and ventilation) of broiler houses. The energy model needs as input data the main thermo-physical and geometrical properties of the house, the farming features and the weather data. The structure of the model is based on five calculation steps as shown in Fig. 5. These steps can be summarized as follow:

a) Boundary conditions calculation: data needed for this calculation were retrieved from technical manuals (regarding animal physiology or environmental control) or from broiler management guides published by broiler selling companies. Through this calculation, the parameters depending on the reared animals are initialized and their weight, their thermal emission, base ventilation flow rate and set point temperatures are expressed as a function of the animal age.

b) Energy balance solution: the simple hourly method of ISO 13790 Standard [18] was customized and applied to predict the indoor conditions at each time step of the analyzed period. The set point values for indoor air temperature and the optimal range of relative humidity are taken from calculation a). The weather data adopted in the model is –usually- the Test Methodological Year (TMY). Solving the energy balance, the simulation model establishes if a heating or a cooling load is needed or if the indoor air temperature is within the acceptability range. If no tunnel ventilation or evaporative cooling is present at a certain time step, calculation steps d) and e) can be applied directly, otherwise next step is calculation c).

c) Tunnel ventilation and evaporative cooling calculation: the theoretical cooling load calculated at b) is used for estimating the airflow rate of tunnel ventilation that must be provided by the fans to cool the house for reaching the cooling set point temperature. The presence of the evaporative cooling is also considered. In order to develop this calculation, the model uses as input data the direct saturation effectiveness (ε) of the evaporative pads and the temperature differential (Δt_{tv}) for the activation of evaporative cooling. Knowing these data, the actual indoor air temperature is obtained by the solution of the energy balance using the updated values of airflow rate and supply air temperature.

d) Moisture balance solution: hourly humidity conditions are computed. Through psychrometric equations, the RH of the air inside the broiler house is calculated. Even though RH has not a strong influence on the energy consumption, it is a fundamental parameter for animal welfare because if RH values are far from the optimal ones during a remarkable span of time, broiler health and production could be seriously compromised.

e) System performance: the last calculation provides actual thermal and electrical energy consumption values. The needed input values come from calculations b) and c). Considering the efficiency of air heaters, the thermal energy consumption for space heating can be estimated. For defining the performance of each considered fan model, two operations were carried out for. Firstly, the provided ventilation flow rate was expressed as function of the static pressure differential between indoor and outdoor environments. Secondly, Specific Fan Performance (SFP), that correlates the airflow with the electrical energy consumption, was calculated. Through these functions and the input from the previous calculation steps, electrical energy consumption due to ventilation (both for base and tunnel ventilation) is calculated. Introducing the specific costs of thermal and electrical energy in the model, the total cost due to climate control can be also obtained as output from this calculation step.

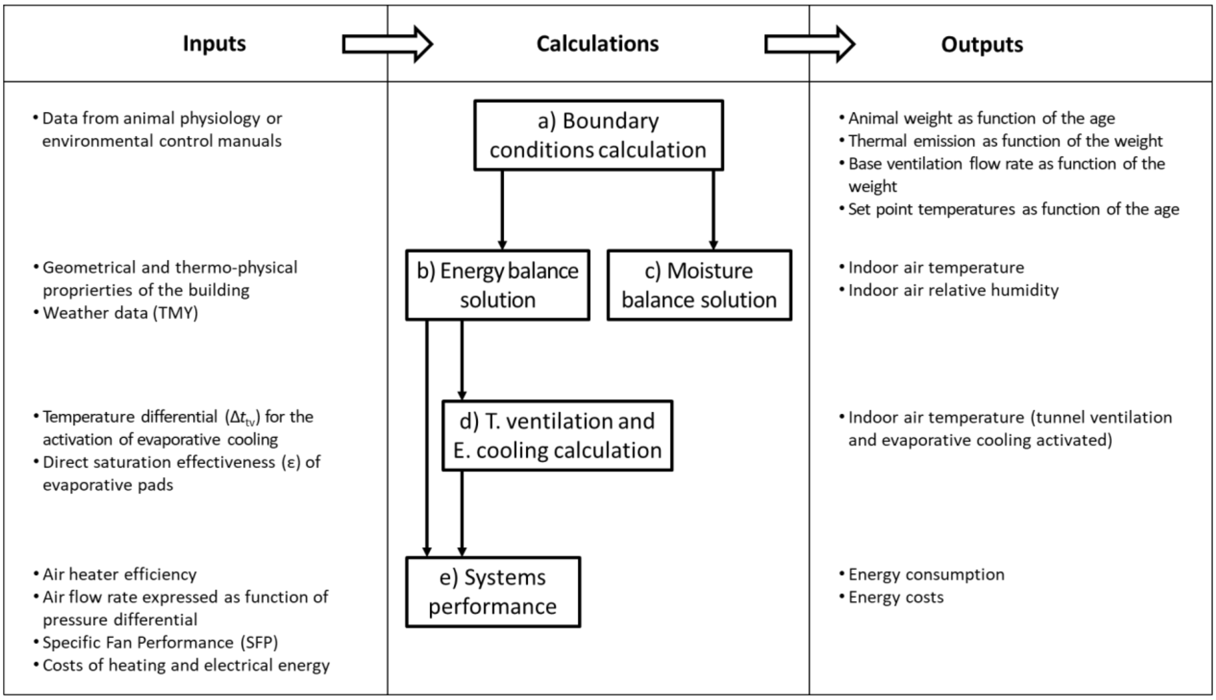

Fig. 5. Scheme of the model structure with inputs and outputs.

3.3 Input data and boundary conditions calculation

Input data concern the geometrical properties of the house (e.g. geometrical dimensions and volume), thermo-physical proprieties (e.g. thermal transmittance) and features of climate control systems (e.g. air heater efficiency and number and models of fans). Other needed data concern weather conditions (e.g. external temperature and solar radiation) and animal production features (e.g. animal stocking density and batch duration). Data regarding the production process are necessary to calculate the yearly schedules of every variable depending on the animals. Through these data, occupancy schedule, animal age, weight, thermal emission and set point temperatures are estimated for each time step of the analyzed period. The needed data used as inputs for the boundary conditions calculation come from technical manuals (regarding physiology or environmental control) [33]-[35] [69] and from broiler management guides [31] [32] [70] [71].
The simulation model calculates the weight of the birds as a function of their age (in days). This function was implemented using values provided by [32] where per each day of broiler age, the expected weight is presented, and reads

$$w_{\mathrm{b}} = f_1 \cdot d^3 + f_2 \cdot d^2 + f_3 \cdot d + f_4 \quad [\mathrm{kg}] \tag{1}$$

where w_b (in kg) is the bird live weight and d (in days) is the bird age. Coefficients f_1, f_2, f_3 and f_4 were determined reducing the last square error from the provided data and their values are presented in Table 1.

Table 1 - Coefficients of Eq. (1) that expresses the broiler weight (w_b) as function of its age (d).

Coefficient	Value	Unit
f_1	$-2.1164 \cdot 10^{-5}$	$kg \cdot day^{-3}$
f_2	$+2.5608 \cdot 10^{-3}$	$kg \cdot day^{-2}$
f_3	$-5.3002 \cdot 10^{-3}$	$kg \cdot day^{-1}$
f_4	$+7.0839 \cdot 10^{-2}$	kg

In broiler farming, the best indoor climate conditions for the animals (indoor air temperature and RH) depend on animal age. Data about ideal climate conditions are present in various broiler management guides. For the development of the presented energy model, data from [71] were used.

Firstly, the indoor air set point temperature $t_{avg,set}$ was obtained as a function of the broiler age. From $t_{avg,set}$, a dead band in which temperature fluctuates in free running conditions was set. The lower value of this band was assumed as heating set point temperature $t_{H,set}$, while the upper one was assumed as cooling set point temperature $t_{C,set}$. In Fig. 6 the trends of the set point values $t_{H,set}$, $t_{C,set}$ and $t_{avg,set}$ during a production cycle are shown together with w_b as a function of the animal age. The chart shows that in the first days of the batch, indoor air temperature set points are higher than in the following days, because animals that are present inside the house are still chicks. During the last part of the batch, heating and cooling set points decrease since older broilers need lower temperatures than chicks.

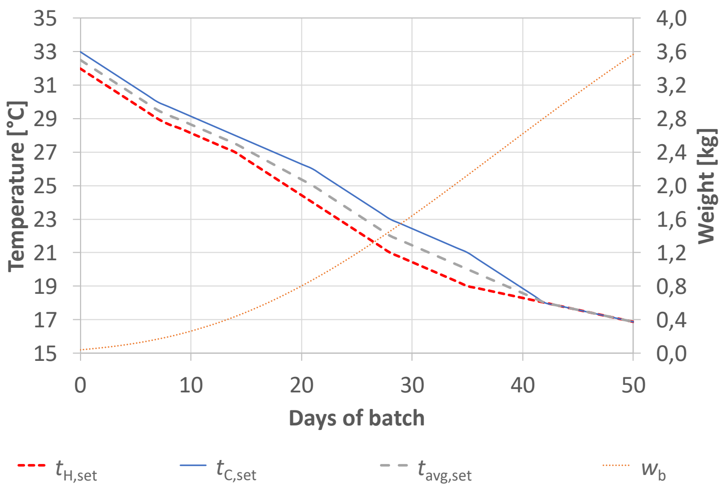

Fig. 6. Trend of heating set point temperature ($t_{H,set}$), cooling set point temperature ($t_{C,set}$) and central set point temperature ($t_{avg,set}$) during a batch. In the chart, animal weight (w_b) is also shown.

Broiler weight calculated by Eq. (1) is used to estimate the animal total heat production. This heat emission has a better correlation with the animal body area rather than with the body weight, but body area per unit of volume or weight is not constant, thus the relationship becomes more complex. For this reason, it is preferred to express the single animal total heat production $\Phi_{\mathrm{b,sens+lat}}$ as a function of to the weight w_{b} [33]. A general application was studied by Brody, as reported in [33] and it reads:

$$\Phi_{\mathrm{b,sens+lat}} = k \cdot w_{\mathrm{b}}^{0.734} \quad [\mathrm{W}] \tag{2}$$

where k is a coefficient that varies depending on animal species. A more recent study [34] gives the following formulation for broilers that was used in the development of this model:

$$\Phi_{\mathrm{b,sens+lat}} = 10 \cdot w_{\mathrm{b}}^{0.75} \quad [\mathrm{W}] \tag{3}$$

Eq. (3) represents the total heat emissions of a broiler, considering both latent and sensible heat emission. The total heat emission of the flock $\Phi_{\mathrm{f,sens+lat}}$ is obtained by multiplying $\Phi_{\mathrm{b,sens+lat}}$ by the number of animals n (an input data) as

$$\Phi_{\mathrm{f,sens+lat}} = \Phi_{\mathrm{b,sens+lat}} \cdot n \quad [\mathrm{W}] \tag{4}$$

The share between sensible and latent heat emission depends on environmental conditions, being the latent heat emission positively correlated with the raise of the temperature, while sensible heat emission decreases with the raise of temperature. The sensible fraction of the heat emission in the enclosure R, is calculated as a function of the central set point temperature $t_{\mathrm{avg,set}}$ as

$$R = b_1 \cdot t_{\mathrm{avg,set}}^6 + b_2 \cdot t_{\mathrm{avg,set}}^5 + b_3 \cdot t_{\mathrm{avg,set}}^4 + b_4 \cdot t_{\mathrm{avg,set}}^3 + b_5 \cdot t_{\mathrm{avg,set}}^2 + b_6 \cdot t_{\mathrm{avg,set}} + b_7 \quad [-] \tag{5}$$

where b coefficients are reported in Table 2 and were determined reducing the last square error on data from [34].

Table 2 - Coefficients of Eq. (5) that expresses the sensible fraction of the heat emission (*R*) as function of the central set point temperature ($t_{avg,set}$).

Coefficient	Value	Unit
b_1	$+1.1570 \cdot 10^{-9}$	$°C^{-6}$
b_2	$+1.1814 \cdot 10^{-7}$	$°C^{-5}$
b_3	$-5.1467 \cdot 10^{-6}$	$°C^{-4}$
b_4	$+9.7688 \cdot 10^{-5}$	$°C^{-3}$
b_5	$-4.8856 \cdot 10^{-4}$	$°C^{-2}$
b_6	$-7.2767 \cdot 10^{-3}$	$°C^{-1}$
b_7	$+6.3921 \cdot 10^{-1}$	-

Knowing the fraction of sensible heat produced, the sensible $\Phi_{b,sens}$ and latent $\Phi_{b,lat}$ heat production of each broiler is calculated as

$$\Phi_{\mathrm{b,sens}} = R \cdot \Phi_{\mathrm{b,sens+lat}} \quad [\mathrm{W}] \tag{6}$$

$$\Phi_{\mathrm{b,lat}} = \Phi_{\mathrm{b,sens+lat}} - \Phi_{\mathrm{b,sens}} \quad [\mathrm{W}] \tag{7}$$

These values are used to obtain the sensible and latent heat emission of the flock, respectively $\Phi_{f,sens}$ and $\Phi_{f,lat}$, as

$$\Phi_{\mathrm{f,sens}} = \Phi_{\mathrm{b,sens}} \cdot n \quad [\mathrm{W}] \tag{8}$$

$$\Phi_{\mathrm{f,lat}} = \Phi_{\mathrm{b,lat}} \cdot n \quad [\mathrm{W}] \tag{9}$$

The vapor mass flow rate of total flock $\dot{m}_{f,v}$ is calculated using the equation

$$\dot{m}_{\mathrm{f,v}} = \frac{\Phi_{\mathrm{b,lat}} \cdot 10^{-3}}{h_{\mathrm{v,i}}} \cdot n \quad \left[\frac{\mathrm{kg}}{\mathrm{s}}\right] \tag{10}$$

where $\Phi_{b,lat}$ is the latent heat production (expressed in W), $h_{v,i}$ is the specific enthalpy of the vapor ($kJ \cdot kg^{-1}$) evaluated at $t_{avg,set}$ and *n* is the flock broiler number (birds).

The high stocking densities typical of broiler houses entail a not negligible vapor production that increases the RH of the indoor air. High levels of RH increase the thermal stress of the animals and worsen the IAQ, together with contaminants present in the air. Range of optimal RH values can be found in literature [34]. In Fig. 7, the optimal RH range values considered in this work are shown together with w_b as a function of the animal age.

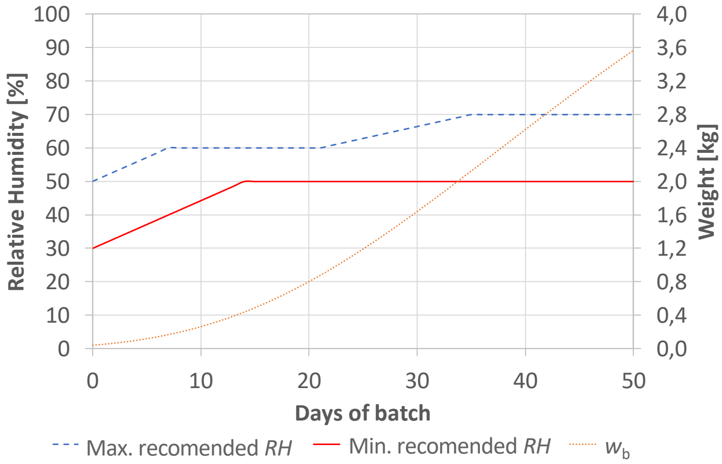

Fig. 7. Optimal RH range values during a batch. In the chart, animal weight (w_b) is also shown..

In broiler houses, mechanical humidification or dehumidification system are not present. The RH is managed through base ventilation only. The air flow rate necessary to maintain IAQ in the house $\dot{V}_{\text{base,tot}}$ is determined as a function of base ventilation flow rate per kg of live weight $\dot{V}_{\text{base,w}}$. This flow rate is calculated as a function of broiler's age *d* through the equation

$$\dot{V}_{\text{base,w}} = g_1 \cdot d^4 + \; g_2 \cdot d^3 + g_3 \cdot d^2 + g_4 \cdot d + g_5 \quad \left[\frac{\text{m}^3}{\text{h} \cdot \text{kg}}\right] \tag{11}$$

where *g* coefficients (showed in Table 3) were obtained through a regression analysis on values from [71].

Table 3 - Coefficients of Eq. (11) that expresses the ventilation flow rate per kg of live weight ($\dot{V}_{\text{base,w}}$) as function of the broiler age (d).

Coefficient	Value	Unit
g_1	$+3.6000 \cdot 10^{-7}$	$m^3 \cdot h^{-1} \cdot kg^{-1} \cdot day^{-4}$
g_2	$-6.6070 \cdot 10^{-5}$	$m^3 \cdot h^{-1} \cdot kg^{-1} \cdot day^{-3}$
g_3	$+4.6223 \cdot 10^{-3}$	$m^3 \cdot h^{-1} \cdot kg^{-1} \cdot day^{-2}$
g_4	$-1.5193 \cdot 10^{-1}$	$m^3 \cdot h^{-1} \cdot kg^{-1} \cdot day^{-1}$
g_5	$+2.4666$	$m^3 \cdot h^{-1} \cdot kg^{-1}$

Knowing $\dot{V}_{\text{base,w}}$, total base ventilation flow rate $\dot{V}_{\text{base,tot}}$ is calculated as

$$\dot{V}_{\text{base,tot}} = \dot{V}_{\text{base,w}} \cdot n \cdot w_{\text{b}} \quad \left[\frac{\text{m}^3}{\text{h}}\right] \tag{12}$$

3.4 *Energy balance*

The calculation model presented in this work complies with the simple hourly method described in ISO 13790 Standard [18] and it is based on a similarity between the thermal behavior of the analyzed building and a resistance–capacitance (R-C) network. This similarity allows a simplification of the heat transfer between the indoor and the outdoor environment. The model consists of five resistances and one capacitance (5R1C), as shown in Fig. 8. Each resistance of the network represents a heat transfer coefficient, while the nodes indicate the various considered temperatures. The heat capacity of the entire building is concentrated in the single capacitance of the 5R1C network.

The heating/cooling load $\Phi_{H/C,nd}$ is applied on the node representing the indoor air temperature t_{air}. The resistance representing the heat transfer coefficient by ventilation H_{ve} is connected to the same t_{air} node. The heat flow rate representing thermal losses by ventilation is calculated as a function of H_{ve} and the temperature difference between the supply air temperature t_{sup} and t_{air}. In this specific model, t_{sup} is assumed equal to the outdoor air temperature t_e when evaporative cooling is not activated. Contrarily, when evaporative pads are activated, outdoor air used for tunnel ventilation is adiabatically saturated and its temperature decreases.

The heat flow rate by transmission through the building envelope depends on the temperature difference between t_e and surface temperature t_s, which is a mix between mean radiant temperature and indoor air temperature and it also depends on the heat transfer coefficients by transmission for glazed elements $H_{tr,fen}$ and for opaque ones $H_{tr,op}$.

In order to correctly consider the thermal mass of the building, the coefficient $H_{tr,op}$ is split, in turn, into two coefficients $H_{tr,em}$ and $H_{tr,ms}$ with a single concentrated thermal capacity C_m between them, as shown in Fig. 8. In this way, the model considers that two different heat flows occur through the opaque elements. The first one represents the heat flow by transmission that takes place between the outdoor environment and the core of the opaque components, where the 5R1C model considers that the building fabric effective heat capacity C_m is located. This part of the heat flow is calculated as a function of $H_{tr,em}$ and the temperature difference between t_e and the capacitive mass node temperature t_m. The second part of the transmission heat flow through the opaque elements represents the heat transfer that takes place between the thermal mass and the indoor environment. This quantity depends on the heat transfer coefficient $H_{tr,ms}$ and on the temperature difference between t_m and t_s. Temperature t_s is connected to t_{air} node through a heat transfer coefficient $H_{tr,is}$, obtainable as the product between the area of all surfaces facing the building zone A_{tot} and the surface heat transfer coefficient h_{is}.

The heat gains due to solar Φ_{sol} and internal sources Φ_{int} are considered split into three different shares (Φ_{ia}, Φ_{m} and Φ_{st}) as visible in Fig. 8. Each one acts on a different node of the R-C network. In the t_{air} node, the Φ_{ia} heat flow is present and it represents the convective part of the heat gains and it is equal to half of the heat gains from internal sources. Φ_{m} represents the heat flow that affects the mass temperature node t_{m} and it is a function of the total radiative heat gains (solar and internal) and of the fraction between the effective mass area of the building A_{m} and the area of all surface facing the enclosure A_{tot}. The remaining part of the radiative internal and solar gains is Φ_{st} that act on the t_{s} node and depends on the same parameters of Φ_{m} and also on the transmission heat transfer coefficient of the windows $H_{tr,fen}$. At each time step, the actual heating/cooling load $\Phi_{H/C,nd}$ that has to be provided directly to the building to reach the heating/cooling set point temperature $t_{H/C,set}$ is calculated. The sum, during the analyzed period, of the hourly heating/cooling load gives as result the total heating/cooling energy need $Q_{H/C,nd}$. Even though this method makes possible the calculation of the cooling energy needs to decrease the indoor air temperature until the cooling set point, in this specific work these data were used only as input to calculate the tunnel ventilation air flow $\dot{V}_{tv}$, because mechanical cooling usually is not present in broiler houses.

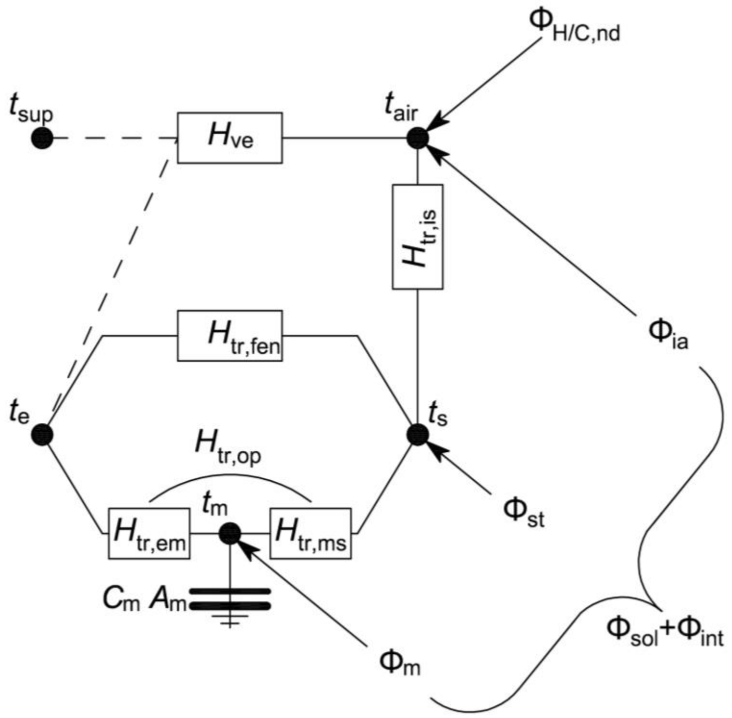

Fig. 8. Representation of the simple hourly model.

To proceed to the calculation of the hourly energy heating/cooling load $\Phi_{H/C,nd}$ applied to the t_{air} node, a time discretization is done following a Crank-Nicholson scheme which analyzes the 5R1C model with an hourly time step. At each time step t_{air} is calculated and compared with set point temperatures $t_{H,set}$ and $t_{C,set}$ and the total heat flow $\Phi_{m,tot}$ that considers all the heat flows occurring in that time step is calculated. To do it, coefficients $H_{tr,1}$, $H_{tr,2}$, $H_{tr,3}$ are needed and are calculated as a function of $H_{tr,fen}$ and H_{ve}. The full set of equations needed for this calculation steps and for the entire calculation of the model, can be found in paragraph C.3 of Annex C of ISO 13790 Standard.

Knowing all the previous quantities, the capacity mass node temperature $t_{m,\tau}$ is calculated, at each time step τ, as

$$t_{\mathrm{m},\tau} = \frac{t_{\mathrm{m},\tau-1} \cdot \left[\frac{C_\mathrm{m}}{3600} - 0.5 \cdot \left(H_{\mathrm{tr},3} + H_{\mathrm{tr,em}}\right)\right] + \Phi_{\mathrm{m,tot}}}{\frac{C_\mathrm{m}}{3600} + 0.5 \cdot \left(H_{\mathrm{tr},3} + H_{\mathrm{tr,em}}\right)} \quad [°\mathrm{C}] \qquad (13)$$

where C_m is the building fabric effective heat capacity (expressed in $J \cdot K^{-1}$) and $t_{m,\tau-1}$ is the capacitive mass node temperature at the previous time step.

Capacitive mass temperature t_m, surface temperature t_s and indoor air temperature t_{air} of the enclosure are calculated at each time step as

$$t_\mathrm{m} = \frac{t_{\mathrm{m},\tau} + t_{\mathrm{m},\tau-1}}{2} \quad [°\mathrm{C}] \qquad (14)$$

$$t_\mathrm{s} = \frac{H_{\mathrm{tr,ms}} \cdot t_\mathrm{m} + \Phi_{\mathrm{st}} + H_{\mathrm{tr,fen}} \cdot t_\mathrm{e} + H_{\mathrm{tr},1} \cdot \left(t_{\mathrm{sup}} + \frac{\Phi_{\mathrm{ia}} + \Phi_{\mathrm{H/C,nd}}}{H_{\mathrm{ve}}}\right)}{H_{\mathrm{tr,ms}} + H_{\mathrm{tr,fen}} + H_{\mathrm{tr},1}} \quad [°\mathrm{C}] \qquad (15)$$

$$t_{\mathrm{air}} = \frac{H_{\mathrm{tr,is}} \cdot t_\mathrm{s} + H_{\mathrm{ve}} \cdot t_{\mathrm{sup}} + \Phi_{\mathrm{ia}} + \Phi_{\mathrm{H/C,nd}}}{H_{\mathrm{tr,is}} + H_{\mathrm{ve}}} \quad [°\mathrm{C}] \qquad (16)$$

where $\Phi_{H/C,nd}$ is the actual heating/cooling load. At each time step, t_{air} is calculated twice, considering firstly no heating/cooling load obtaining $t_{air,0}$ and then an heating/cooling load equal to 10 $W \cdot m^{-2}$ ($\Phi_{H/C,nd,10}$ obtaining $t_{air,10}$). The actual heating/cooling load $\Phi_{H/C,nd}$ is determined as

$$\Phi_{\mathrm{H/C,nd}} = \Phi_{\mathrm{H/C,nd,10}} \cdot \frac{t_{\mathrm{int,H/C,set}} - t_{\mathrm{air},0}}{t_{\mathrm{air},10} - t_{\mathrm{air},0}} \quad [\mathrm{W}] \qquad (17)$$

Two different conditions that can occur in the broiler house have to be considered at each time step. The first one happens when $t_{air,0}$ falls between the heating $t_{H,set}$ and cooling set point temperatures $t_{C,set}$, therefore the building does not need neither heating nor cooling ($\Phi_{H/C,nd}$=0) and the temperature is in free-floating conditions. The second condition happens when $t_{air,0}$ falls out of the range fixed by the two indoor air temperature set points and a heating/cooling load $\Phi_{H/C,nd}$ is registered. Considering all the hourly heating/cooling loads (given by Eq. (17)), the total energy needs during the considered period are obtained. The heating load is stored for calculation of the heating energy use, while the cooling load is simply theoretical and it is used for the following tunnel ventilation calculations.

3.5 Tunnel ventilation and evaporative cooling

As reported before, mechanical cooling is not present in broiler houses, but free cooling can be activated to decrease the indoor air temperature through the tunnel ventilation.
From the previous calculation steps, the building loads and the boundary conditions at each time step are known. The model considers that tunnel ventilation is activated when all the following conditions are fulfilled:

a) broilers are present in the house;
b) the house has to be cooled (t_{air}>$t_{C,set}$ and $\Phi_{H/C,nd}$ is negative);
c) t_e is sufficiently lower than $t_{C,set}$.

The last condition has to be imposed because for cooling the indoor environment through tunnel ventilation, t_e has to be lower than $t_{C,set}$ of a certain temperature differential Δt_{tv}. This condition can be expressed as

$$t_{\mathrm{C,set}} - t_{\mathrm{e}} \geq \Delta t_{\mathrm{tv}} \tag{18}$$

where Δt_{tv} is the minimum difference between $t_{C,set}$ and t_e for activating tunnel ventilation. This parameter is set in the climate control unit and generally varies between 0.5 and 3 °C. In the presented model Δt_{tv} is a constant input data.
When all the previous conditions are verified, the tunnel ventilation flow rate $\dot{V}_{tv}$ is calculated as

$$\dot{V}_{\mathrm{tv}} = \frac{\left|\Phi_{\mathrm{C,nd}}\right|}{c_{\mathrm{air}} \cdot \left(t_{\mathrm{C,set}} - t_{\mathrm{e}}\right)} \cdot \frac{3600}{\rho_{\mathrm{air}}} \quad \left[\frac{\mathrm{m}^3}{\mathrm{h}}\right] \tag{19}$$

where c_{air} is the specific heat capacity of the air and ρ_{air} is air volumetric mass density.
Δt_{tv} is also a condition that guarantees the feasibility of the ventilation, as it stands out from Eq. (18). If the difference between $t_{C,set}$ and t_e is close to zero, the requested ventilation flow rate increases, reaching excessively high values that are not feasible or that entail air velocities not adequate for the welfare of broilers.
Given a maximum theoretical cooling load, a small value of Δt_{tv} entails a maximum flow rate of tunnel ventilation larger than the one that may be obtained assuming a greater value of Δt_{tv}.
The maximum value of the tunnel ventilation flow rate $\dot{V}_{tv,max}$ is

$$\dot{V}_{\mathrm{tv,max}} = \frac{\left|\Phi_{\mathrm{C,nd,max}}\right|}{c_{\mathrm{air}} \cdot \Delta t} \cdot \frac{3600}{\rho_{\mathrm{air}}} \quad \left[\frac{\mathrm{m}^3}{\mathrm{h}}\right] \tag{20}$$

where $\Phi_{C,nd,max}$ is the maximum cooling load needed. Knowing $\dot{V}_{tv,max}$ and the geometrical dimensions of the house, the maximum air velocity in the house due to ventilation is calculated. This parameter is useful for analyzing the animal welfare during the batch.
During the warmest periods, t_e may rise above the cooling set point temperature $t_{C,set}$, therefore Eq. (18) is not fulfilled.
When this situation happens, tunnel ventilation cannot maintain the indoor air temperature set point and high temperature peaks may be reached. To guarantee the animal health and to safeguard the production in these periods too, direct evaporative cooling is activated. This strategy reduces the supply air temperature and it cools the enclosure.
The model considers that direct evaporative cooling is activated when all the following conditions are verified:

- broilers are present in the house;
- a cooling load is needed;
- the condition of Eq. (18) is not fulfilled (t_e is not sufficiently lower than $t_{C,set}$);
- the livestock house is equipped with evaporative pads.

When evaporative cooling is activated, evaporative pads cool the outdoor air that passes through them by adiabatic saturation. The t_{sup} value is determined as a function of t_e, the outdoor humidity (expressed through the wet-bulb temperature) and the direct saturation effectiveness ε of the cooling pad. Saturation effectiveness indicates the extent to which complete saturation is approached [11] that is the percentage of the closeness between the dry-bulb temperature of the air leaving the cooling pad $t_{sup,db}$ and the wet-bulb temperature of the entering air $t_{e,wb}$. Generally, ε varies between 70 and 95% as a function of the air velocity through the pad (values between 1.0 and 1.4 m·s^{-1} produce the highest efficiencies [36]), the thickness of the pad (between 10 and 30 cm) [11] and the maintenance (dust, particles and algae decrease the efficiency). In a generic cooling pad, ε can be expressed as

$$\varepsilon = 100 \cdot \frac{t_{e,db} - t_{sup,db}}{t_{e,db} - t_{e,wb}} \;\; [\%] \tag{21}$$

where $t_{e,db}$ is the dry-bulb temperature of the entering air.
When evaporative cooling is activated, the model determines t_{sup} as

$$t_{sup,db} = t_{e,db} - \varepsilon \cdot \left(t_{e,db} - t_{e,wb}\right) \;\; [°C] \tag{22}$$

When evaporative cooling is activated, the tunnel ventilation flow rate $\dot{V}_{tv,ec}$ is updated as

$$\dot{V}_{tv,ec} = \frac{\left|\Phi_{C,nd}\right|}{c_{air} \cdot \left(t_{C,set} - t_{sup}\right)} \cdot \frac{3600}{\rho_{air}} \;\; \left[\frac{m^3}{h}\right] \tag{23}$$

The indoor air temperature calculations at each analyzed time step is updated and the equations concerning the energy balance (Eq. (13) and following) are recalculated considering the tunnel ventilation flow rates with/without the evaporative cooling.
After this last step, the model is able to report the correct values of t_{air} also in those time steps in which ventilation and evaporative cooling are activated.

3.6 Moisture balance

The energy model solves the humidity mass balance, for each analyzed time step. This balance considers humidity ratio of indoor air x_i and supply air x_{sup} and the vapor production flow rate of the flock $\dot{m}_{f,v}$, as shown in Fig. 9. The properties of moisture storage of the envelope, the animals' plumage and the straw present in the litter are not considered in the present work. The humidity mass balance can be expressed as

$$\dot{V}_{eff} \cdot \rho_{air} \cdot \left(x_{sup} - x_i\right) + \dot{m}_{f,v} \cdot 3600 = 0 \;\; \left[\frac{kg_v}{h}\right] \tag{24}$$

where $\dot{V}_{eff}$ is the effective ventilation flow rate inside the house, equal to $\dot{V}_{base,tot}$ when only base ventilation is activated, $\dot{V}_{tv}$ when tunnel ventilation is activated and $\dot{V}_{tv,ec}$ when evaporative cooling is activated. The balance expressed in Eq. (24) is solved in order to determine x_i.

Through standard psychrometric formulations, the model provides as output the RH of the indoor air. This parameter is of the foremost importance in broiler farming because it makes possible to understand if the base ventilation flow rate is adequate to guarantee the animal comfort avoiding too high or too low levels of RH that can cause animal stress and diseases [72].

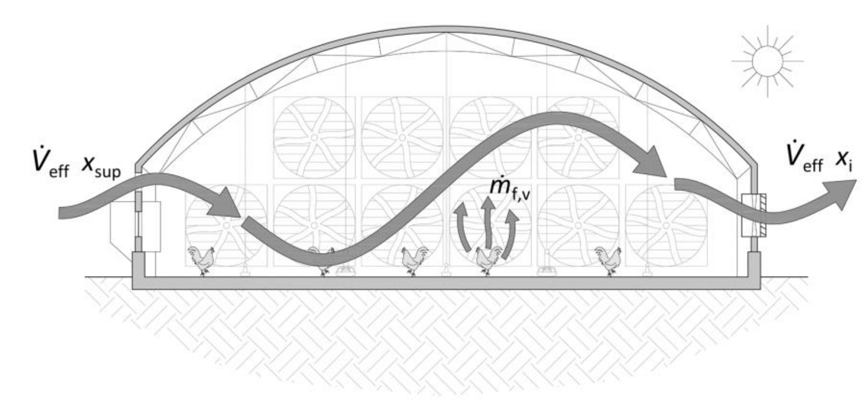

Fig. 9. Humidity mass balance solved by the simulation model.

3.7 Systems performance

In the previous sections, the calculations for estimating the energy needs for heating, cooling and ventilation were shown. For obtaining the thermal and electrical energy consumption due to climate control, the performance of the systems installed in the house has to be computed. Air heaters carry out the heating task. They are equipped with a fuel burner with a certain conversion efficiency η. The heating energy consumption is calculated as

$$E_{\mathrm{th}} = Q_{\mathrm{H,nd}} \cdot \eta \;\; [\mathrm{kWh}] \tag{25}$$

where $Q_{\mathrm{H,nd}}$ is the energy needs for heating, calculated as the sum of the heating load for each time step of the analyzed period.

To estimate the electrical energy consumption of the fans for both base and tunnel ventilation, the model considers the static pressure p in the house (calculated as the difference between inside and outside pressure) at each analyzed time step.

Three different situations may occur. The first one includes those time steps in which the tunnel ventilation is not activated. In this situation, the static pressure of the air into the broiler house corresponds to the static pressure due to the base ventilation p_{bs}, a parameter input by the user, therefore

$$p = p_{\mathrm{bs}} \;\; [\mathrm{Pa}] \tag{26}$$

The second case contemplates the tunnel ventilation as activated, while the evaporative cooling is not activated: in this case, static pressure p_{tv} is calculated as a function of the air velocity v and the length of the broiler house L as [70]:

$$p = p_{\mathrm{tv}} = (2.57 \cdot 10^{-2} \cdot v^2 + 3.1 \cdot 10^{-3} \cdot v + 6 \cdot 10^{-3}) \cdot L \ \ [\mathrm{Pa}] \tag{27}$$

When evaporative cooling is activated, the static pressure is calculated as in Eq. (27), but a further pressure drop of 20 Pa due to the presence of the evaporative cooling pads has to be added to the final result.

In this work, different commercial fans were considered both for base and tunnel ventilation. All those products were tested by laboratories. Through those tests, the air flow rate and the specific electrical consumption of the fans are expressed as a function of the static pressure inside the broiler house (from 0 to 60 or 75 Pa). For estimating the hourly ventilation flow rate $\dot{V}_{fan}$ of a fan present in the house, the following equation is adopted

$$\dot{V}_{\mathrm{fan}} = B_2 \cdot p^2 + B_1 \cdot p + B_0 \ \ \left[\frac{\mathrm{m}^3}{\mathrm{h}}\right] \tag{28}$$

where p is the static pressure value and B_0, B_1 and B_2 are regression coefficients obtained from data obtained by laboratory tests, different for each fan model.

To calculate the electrical energy consumption due to ventilation, a *Specific Fan Performance* (SFP) curve, typical for each fan, is implemented. The SFP curve expresses the energy consumption per each m^3 of airflow provided by the fan and it is a function of the static pressure p as

$$\mathrm{SFP} = S_2 \cdot p^2 + S_1 \cdot p + S_0 \ \ \left[\frac{\mathrm{m}^3}{\mathrm{Wh}}\right] \tag{29}$$

where S_0, S_1 and S_2 are regression coefficients different for each fan.

The model considers that when a base ventilation flow rate $\dot{V}_{base,t}$ or a tunnel ventilation flow rate $\dot{V}_{tv}$ is needed, the first fan assigned to that specific task (base or tunnel ventilation) starts to work providing the ventilation flow rate calculated through Eq. (28). If the ventilation flow rate needed is greater than the one provided by the first fan, the model allocates the remaining ventilation flow rate sequentially to the following fans. For calculating the global electrical energy consumption due to ventilation E_{el} in the broiler house, the sum of the energy consumption of each fan has to be considered and it has to be integrated on the considered interval of time steps τ as

$$E_{\mathrm{el}} = \int_{\tau}^{0} \left(\sum_{k=1}^{n} \left(\frac{\dot{V}_{\mathrm{fan,k}}}{\mathrm{SFP_k}} \right) \cdot 10^{-3} \right) d\tau \quad [\mathrm{kWh}] \tag{30}$$

where n is the number of fans present into the broiler house.
Through these calculations, the thermal and electrical energy consumption due to climate control in the broiler house are finally obtained.

4 Validation of the model

The presented model was calibrated and validated by a comparison with a real dataset obtained through a measurement campaign carried out in a real broiler house. The monitoring campaign concerned an entire production cycle.

4.1 Case study description

The analyzed case study is a gable roof broiler house located in North of Italy. The building has a useful floor area of 1200 m^2, being 120 m long and 10 m wide. The height of the house is 4.4 m at the ridge level and decreases until 2.1 m at the eave level. The useful volume is about 3900 m^3. The main orientation of the building is East-West due to its longest axis is aligned on the north-south direction.
Walls are prefabricated sandwich panels made up of a double layer of prepainted steel sheets with a high density spread polyurethane layer (0.04 m of thickness) interposed. The mean U-value of walls is 0.81 W·m^{-2}K^{-1}. This value is obtained considering that a part of the opaque envelope (about 6% of the north and south walls) is made of corrugated cellulose evaporative pads that are characterized by a higher U-value. The windows are polycarbonate alveolar panels with a U-value of 3.60 W·m^{-2}K^{-1}. The roof is composed by the same prefabricated panels used for the walls, but the interposed polyurethane layer is 0.02 m thick, thus giving a U-value of 1.17 W·m^{-2}K^{-1}. The floor is a reinforced concrete screed above a waterproofing sheet in direct contact with the ground. The effect of the ground was taken into consideration by adding to the original construction of the floor a 1.5 m layer of soil and adopting the outdoor air temperature as the outdoor boundary condition. The internal heat capacity of the opaque elements was calculated following ISO 13786 Standard [73].The main thermo-physical properties of the analyzed broiler house are summarized in Table 4.

Table 4 – Main thermo-physical properties of the analyzed broiler house.

Element	U-value [W·m^{-2}·K^{-1}]	κ_i [kJ·m^{-2}·K^{-1}]
Walls	0.81	4.7
Roof	1.17	4.0
Floor	0.94	79.9
Windows	3.60	-

The batches carried out in the house have a duration of 50 days and the average final live weight achieved by the bird is 3.7 kg. The mean animal stocking density is 12 broilers per square meter of usable floor area, meaning that about 14,500 animals are reared per batch. The ventilation system consists in ten fans of the same model that are located on the south wall and deal with both IAQ control (base ventilation) and tunnel ventilation. In Table 5, *B* and *S* coefficients (Eq. (28) and (29)) of the adopted fan model are reported. Five gas air heaters placed on the north wall of the house provide the space heating. Each gas heater has a 10 kW heating capacity.

Table 5 - Coefficients *B* and *S* of the fans used in the analyzed broiler house.

Coefficient	Value	Unit
B_2	-0.0007	m^3·Pa^{-2}·Wh^{-1}
B_1	-0.2116	m^3·Pa^{-1}·Wh^{-1}
B_0	+34.481	m^3·Wh^{-1}
S_2	-0.8644	m^3·Pa^{-2}·h^{-1}
S_1	-135.04	m^3·Pa^{-1}·h^{-1}
S_0	+42088.5	m^3·h^{-1}

4.2 Monitoring system description

The dataset used for the model calibration and validation concerns both environmental and energy measurements obtained during a single production cycle carried out in May and June that lasted 50 days (1200 hours). The considered period results adequate for the model validation and calibration because during the analyzed batch all the equipment for climate control were used (gas air heaters, fans and evaporative pads).

The environmental data were collected using portable data loggers, which provide the following outputs (accuracy noted in brackets):

1. Indoor air temperature (±0.21 °C);

2. Relative humidity (±2.5%).

The considered broiler house was equipped with two data loggers: the first one placed at the beginning of the house (DL_{Head}) and the second one placed at its end (DL_{Bottom}). Both the devices were installed at 35 cm of height from the floor level. The data acquisition time step was set up to 2 minutes.

Other environmental data were obtained from the climate control unit (CCU) of the house that measures indoor air temperature and RH values with the aim of regulating the fan operations. The maximum (CCU_{Max}), minimum (CCU_{Min}) and medium (CCU_{Med}) daily values of indoor air temperature and RH that are stored by the climate control unit were also used for the calibration and validation stage.

Outdoor air temperature and RH were obtained through a portable data logger (DL_{Out}) arranged outside the broiler house. Hourly solar radiation values were derived from a weather station located near the broiler house.

The monitoring of the energy use for climate control was done as follows. To monitor the thermal energy for heating, the daily working time of each gas air heater was retrieved from CCU. Electrical energy data were obtained through meters for three phase electrical systems that were installed in the electrical line the fans, thus providing the cumulative electrical energy consumption. In Table 6, the dataset obtained through the monitoring campaign is summarized.

Table 6 – Dataset obtained during the monitoring campaign.

Name	Description	Number of samples	Logging time step
DL_{Head}	Indoor air temperature and RH	36,000	2 minutes
DL_{Bottom}	Indoor air temperature and RH	36,000	2 minutes
DL_{Out}	Outdoor air temperature and RH	36,000	2 minutes
CCU_{Max}	Indoor air temperature and RH	50	1 day
CCU_{Min}	Indoor air temperature and RH	50	1 day
CCU_{Med}	Indoor air temperature and RH	50	1 day
Working minutes (gas heaters)	Working time of single gas heater	250	1 day
Energy consumption	Energy consumption of fans	1	50 days (cumulative)

From the whole dataset presented in Table 6, the parameters needed for the calibration and validation of the presented model were obtained. First, the average hourly air temperatures and RH inside the house ($DL_{\mathrm{Average(h)}}$) were obtained as hourly mean between DL_{Head} and DL_{Bottom}. $DL_{\mathrm{Average(d)}}$ was obtained as daily mean of the values of $DL_{\mathrm{Average(h)}}$. Among the parameters obtained from CCU, only CCU_{Med} was used for the validation on a daily basis because it represents the average daily conditions inside the analyzed broiler house.

4.3 Model reliability

The case study previously descripted was simulated to validate and calibrate the presented model. In Fig. 10, daily estimated values from the model ($t_{\mathrm{Model(d)}}$ and $RH_{\mathrm{Model(d)}}$), monitored values from the monitoring system ($t_{\mathrm{DLAverage(d)}}$ and $RH_{\mathrm{DLAverage(d)}}$) and climatic control unit values (t_{CCUMed} and RH_{CCUMed}) are displayed with outdoor air temperature and RH values ($t_{\mathrm{DLOut(d)}}$ and $RH_{\mathrm{DLOut(d)}}$).

Analyzing the trend of the daily outdoor air temperatures, the considered period results relevant for the model validation, as previously said. The first part of the batch is characterized, in fact, by lower outdoor air temperatures (the minimum value is 15.7 °C, measured on the 18$^{\mathrm{th}}$ day of the batch). This value, jointly with the presence of the few-days old chicks in the house, entails a heating need for maintaining the required set point temperatures. During the second part of the analyzed batch, the higher outdoor air temperatures (the maximum value is 29.0 °C measured on the 31$^{\mathrm{st}}$ day of the batch), together with the increased heat production of heavier birds, entails the necessity to cool the animals through the activation of both tunnel ventilation and evaporative cooling. The trends of indoor air temperatures are similar between them, while some differences between RH trends stand out. In particular, RH values estimated by the model ($RH_{\mathrm{Model(d)}}$) are higher than the monitored values ($RH_{\mathrm{DLAverage(d)}}$, RH_{CCUMed}) during 49 out of 50 days of the monitoring campaign (the only exception is day 22). Considerable differences between monitored and estimated values of RH stand out especially in the second part of the analyzed batch, when cooling is needed. For this reason, the deviation between the trends of RH may be due to the evaporative pads modeling. This cooling system has a considerable influence on the RH because it saturates the incoming air, increasing its vapor content. In the model, ε values from the datasheet provided by the manufacturer were used. This value represent the saturation effectiveness of a new pad and tends to decrease over its lifetime as a result of the degradation of the material due to factors as dust, solar radiation and chemical components present in the water used to wet the pad. Considering those aspects, saturation effectiveness may be used as a calibration parameter.

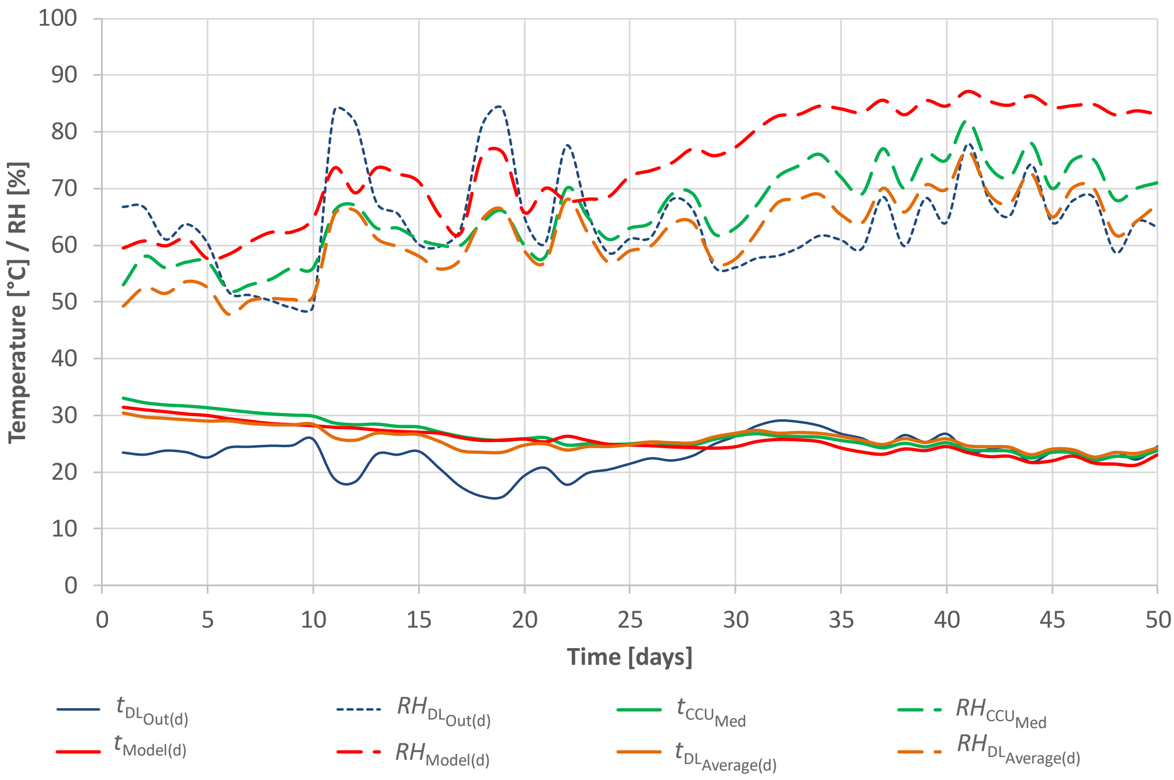

Fig. 10. Trends of daily air temperature and RH of monitored values ($t_{DLAverage(d)}$, $RH_{DLAverage(d)}$, t_{CCUMed} and RH_{CCUMed}) and estimated values ($t_{Model(d)}$ and $RH_{Model(d)}$). In the chart, the monitored outdoor conditions ($t_{DLOut(d)}$ and $RH_{DLOut(d)}$) of air temperature and *RH* are also shown.

In Fig. 11 the hourly trend of indoor air temperature and RH estimated by the model $t_{Model(h)}$ and $RH_{Model(h)}$ are compared with the monitored values $t_{DLAverage(h)}$ and $RH_{DLAverage(h)}$. In the same chart, the hourly total ventilation flow rate (base ventilation plus tunnel ventilation) estimated by the model is also presented. During the first days of the batch, the ventilation flow rate is at a minimum level because the fans are activated only for guaranteeing an acceptable level of IAQ. Being the ventilation for IAQ control a function of the animal weight (as shown in Eq. (11) and Eq. (12)), its flow rate is low during the first days of the batch because in that period tiny chicks are present in the house. As time goes on, the ventilation flow rate increases because heavier birds require higher air flow rates for the IAQ control and because free cooling is needed due to the higher outdoor air temperature values.

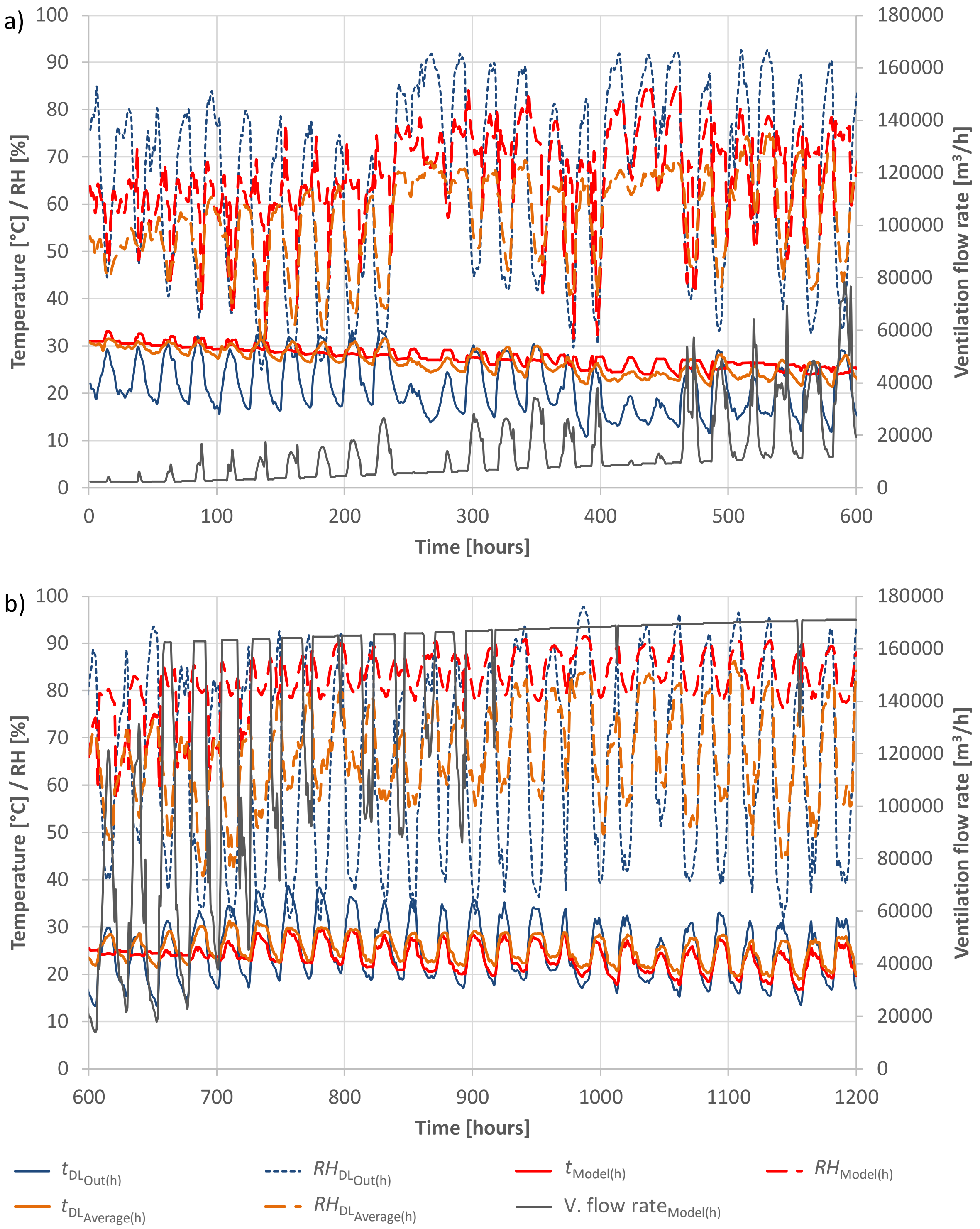

Fig. 11. Trends of hourly indoor air temperature and RH of monitored values ($t_{DLAverage(h)}$ and $RH_{DLAverage(h)}$) and estimated values ($t_{Model(h)}$ and $RH_{Model(h)}$) a) from batch start to hour 600, b) from hour 601 to batch end. In the chart, the monitored outdoor conditions ($t_{DLOut(h)}$ and $RH_{DLOut(h)}$) of air temperature and RH are also shown. The ventilation flow rate estimated by the model is presented.

The goodness-of-fit of the presented model is numerically evaluated using as statistical indexes the Root Mean Square Error (RMSE), the Mean Bias Error (MBE) and the

Coefficient of variation of the Root Mean Square Error (Cv(RMSE)) as done in similar works [74][75][77]. These statistical indexes are calculated as:

$$\mathrm{RMSE} = \sqrt{\frac{\sum_{\mathrm{i}=1}^{N_\mathrm{i}} (M_\mathrm{i} - S_\mathrm{i})^2}{N_\mathrm{i}}} \tag{31}$$

$$\mathrm{MBE} = \frac{\sum_{\mathrm{i}=1}^{\mathrm{N_i}} (M_\mathrm{i} - S_\mathrm{i})}{\sum_{\mathrm{i}=1}^{\mathrm{N_i}} M_\mathrm{i}} \cdot 100 \quad [\%] \tag{32}$$

$$\mathrm{Cv(RMSE)} = \frac{\mathrm{RMSE}}{\frac{1}{N_\mathrm{i}} \sum_{\mathrm{i}=1}^{\mathrm{N_i}} M_\mathrm{i}} \cdot 100 \quad [\%] \tag{33}$$

where M_i and S_i are respectively measured and simulated data at instance i and N_i is the count of the number of values used in the calculation (1200 hourly values, 50 daily values). RMSE is used because it measures the error between simulated and measured data. MBE and Cv(RMSE) are also used for the calibration because their values can be compared with threshold limits provided by ASHRAE Guideline 14 [78] on calibration of building energy models that are equal to ±10% for MBE and 30% for Cv(RMSE) in case of hourly calibrations.

Applying Eq. (30), (31) and (32), RMSE, MBE and Cv(RMSE) values for indoor air temperature and RH were calculated using hourly values ($DL_{\mathrm{Average(h)}}$). RSME is 2.01 °C for indoor air temperature and 16.00% for the RH. MBE for indoor air temperature calculated on hourly basis is 1.30%, while Cv(RMSE) is 7.76%. The same indexes calculated for RH result to be -20.49% (MBE) and 25.85% (Cv(RMSE)). Comparing these values (MBE and Cv(RMSE)) with the reference ones provided by [78], they result to be plenty below the threshold limits concerning the indoor air temperature, but the same situation does not happen for MBE referred to RH values, as shown in Table 7 (columns 3-5, rows 2-4).

On daily interval only RMSE is calculated because ASHRAE Guideline 14 [78] does not provide threshold limits of MBE and Cv(RMSE) for daily calibrations. RMSE on daily basis can be calculated considering as measured data both values from data loggers ($DL_{\mathrm{Average(d)}}$) and from climate control unit (CCU_{Med}), (Table 7, columns 3-5, rows 5-8).

The analysis based on statistical indexes provides useful information: firstly, the model can be considered reliable concerning its previsions about indoor air temperature, the discrepancies of RH may be explained calibrating the saturation effectiveness of the evaporative pads. Secondly, the RMSE shows that the model outputs are more similar to the values provided by the CCU than the ones monitored through portable data loggers.

4.4 Model Calibration

For increasing the reliability of the model, especially concerning the RH values, the direct saturation effectiveness of the evaporative pads was calibrated. This calibration makes it possible to take into account the saturation effectiveness decay of the pads as effect of the variation of the inlet air speed and the deterioration of the materials, as said in the previous section. For the calibration of this parameter, an optimization-based calibration [74] through a GRG (Generalized Reduced Gradient) nonlinear algorithm was adopted for minimizing the RMSE varying the value of ε. The algorithm provides a new value of ε equal to 0.60, instead of 0.87 (initial value) that means a decay of performance by 30%.

In Fig. 12 and Fig. 13, same trends and values of Fig. 10 and Fig. 11 are compared adopting the saturation effectiveness obtained through the calibration process. Both in the hourly and in the daily charts, in facts, the RH values estimated by the model better fit with the measured data. This change can be noticed only in the second part of the batch because evaporative pads were used only during those days.

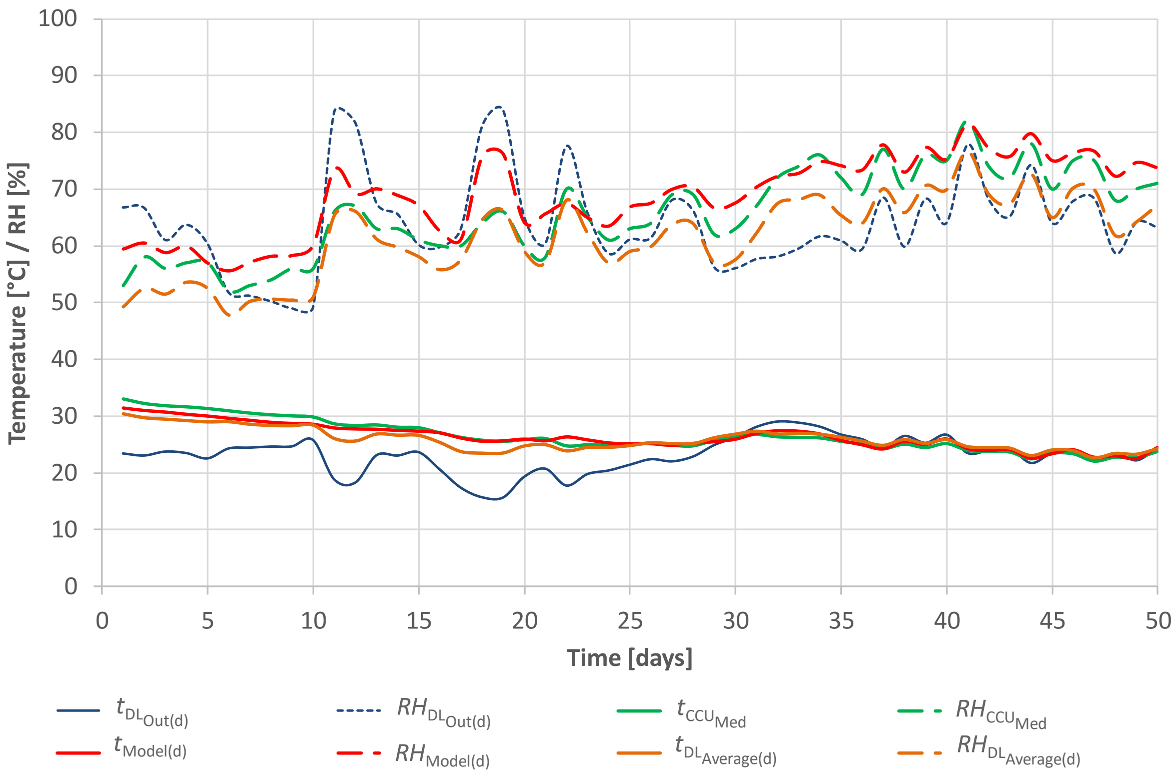

Fig. 12. Trends of daily air temperature and RH of monitored values ($t_{\mathrm{DLAverage(d)}}$, $RH_{\mathrm{DLAverage(d)}}$, t_{CCUMed} and RH_{CCUMed}) and estimated values ($t_{\mathrm{Model(d)}}$ and $RH_{\mathrm{Model(d)}}$) after the model calibration. In the chart, the monitored outdoor conditions ($t_{\mathrm{DLOut(d)}}$ and $RH_{\mathrm{DLOut(d)}}$) of air temperature and RH are also shown.

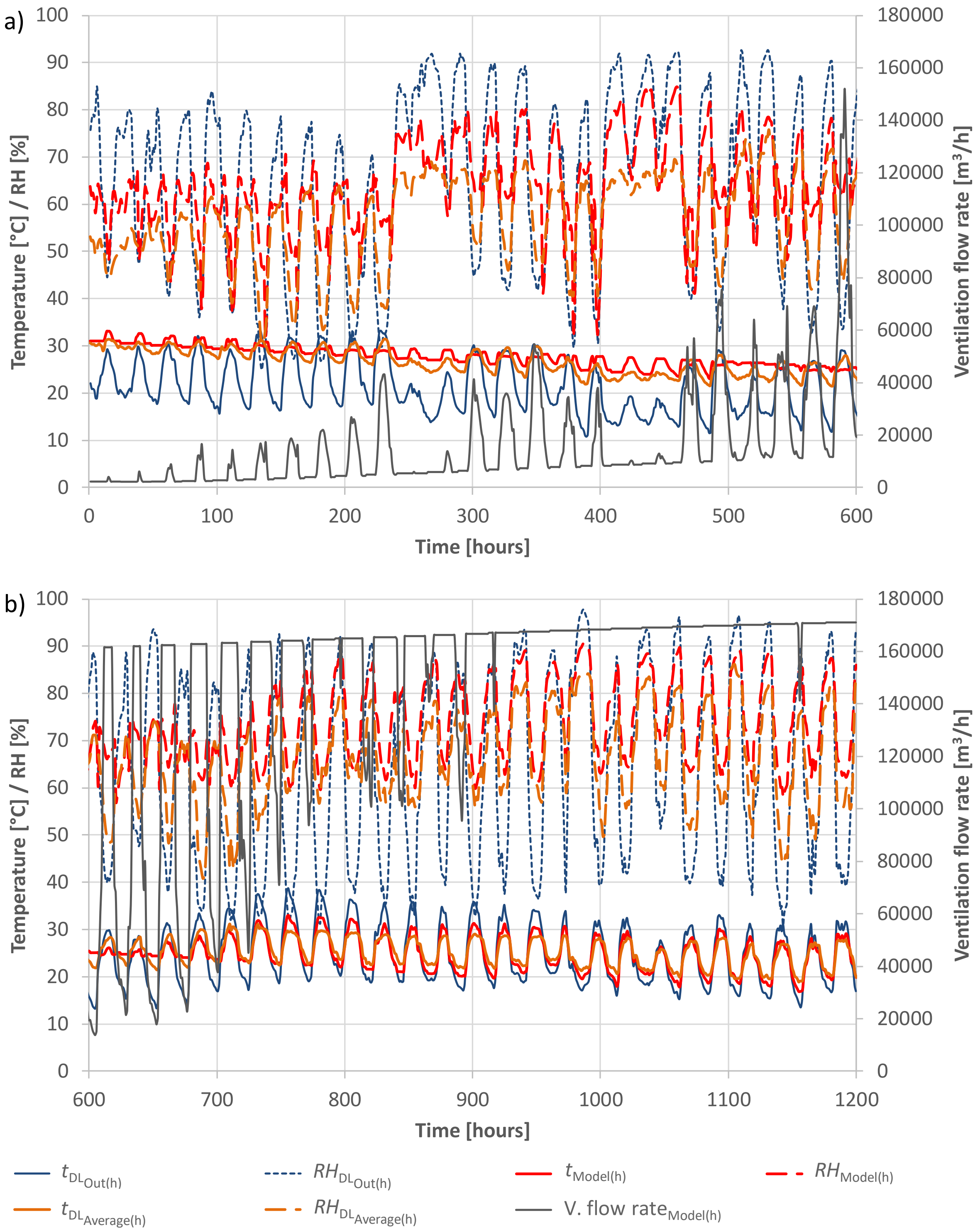

Fig. 13. Trend of hourly indoor air temperature and RH of monitored values ($t_{DLAverage(h)}$ and $RH_{DLAverage(h)}$) and estimated values ($t_{Model(h)}$ and $RH_{Model(h)}$) after the model calibration a) from batch start to hour 600, b) from hour 601 to batch end. In the chart, the monitored outdoor conditions ($t_{DLOut(h)}$ and $RH_{DLOut(h)}$) of air temperature and RH are also shown. The ventilation flow rate estimated by the model is presented.

The increased goodness-of-fit of the model is also proved by the variation of the statistical indexes previously calculated (Table 7, columns 6-9, rows 2-4). Adopting the updated values, the RSME for hourly values of indoor air temperature decreases until 1.65 °C and decreases until 9.38% for RH (logger accuracy was ±0.21 °C for temperature and ±2.5% for RH). The new values of MBE and Cv(RMSE) calculated for indoor air temperature and RH confirm that the reliability of the model has increased, even if the MBE calculated for RH is slightly above the threshold limits, as shown in Table 7. Daily RMSE are also updated (Table 7, columns 6, rows 5-8).

Table 7 – Comparison between the statistical indexes calculated for evaluating the goodness-of-fit of the model and of the calibrated version considering measured (M_i) and simulated values (S_i). The table shows also the threshold limits fixed by ASHRAE Guideline 14 [78].

	M_i	S_i	Model (ε = 0.87)			Calibrated model (ε = 0.60)		
			RMSE	MBE	Cv(RMSE)	RMSE	MBE	Cv(RMSE)
Hourly basis	$t_{DLAverage(h)}$	$t_{Model(h)}$	2.01 °C	1.30%	7.76%	1.65 °C	-1.51%	6.35%
	$RH_{DLAverage(h)}$	$RH_{Model(h)}$	16.00%	-20.49%	25.85%	9.38%	-11.73%	15.19%
	Threshold [78]		-	±10%	30%	-	±10%	30%
Daily basis	$t_{DLAverage(d)}$	$t_{Model(d)}$	1.46 °C	-	-	0.99 °C	-	-
	$RH_{DLAverage(d)}$	$RH_{Model(d)}$	13.47%	-	-	7.59%	-	-
	t_{CCUMed}	$t_{Model(d)}$	1.13 °C	-	-	0.78 °C	-	-
	RH_{CCUMed}	$RH_{Model(d)}$	9.44%	-	-	4.21%	-	-

In order to explain the performance of the model as regard to the RH estimation, an analysis of the residual values (ΔRH) calculated as the hourly difference between S_i and M_i was done, and it is shown in Fig. 14. This distribution has its peak translated on the right part of the chart, meaning that the model constantly overestimates the RH, in fact, 88% of the hourly estimated values ($RH_{Model(h)}$) are greater than monitored values ($RH_{DLAverage(h)}$). This distribution suggests a sort of systematic error of the model that may be due to the hygric material property. The model, in fact, does not take into account that the vapor content present in the air is partially absorbed by the animal plumage and the bedding straw, decreasing the vapor content of indoor air. Further developments of the model may take into account the hygroscopicity of the indoor environment for obtaining a better prediction of the indoor air RH.

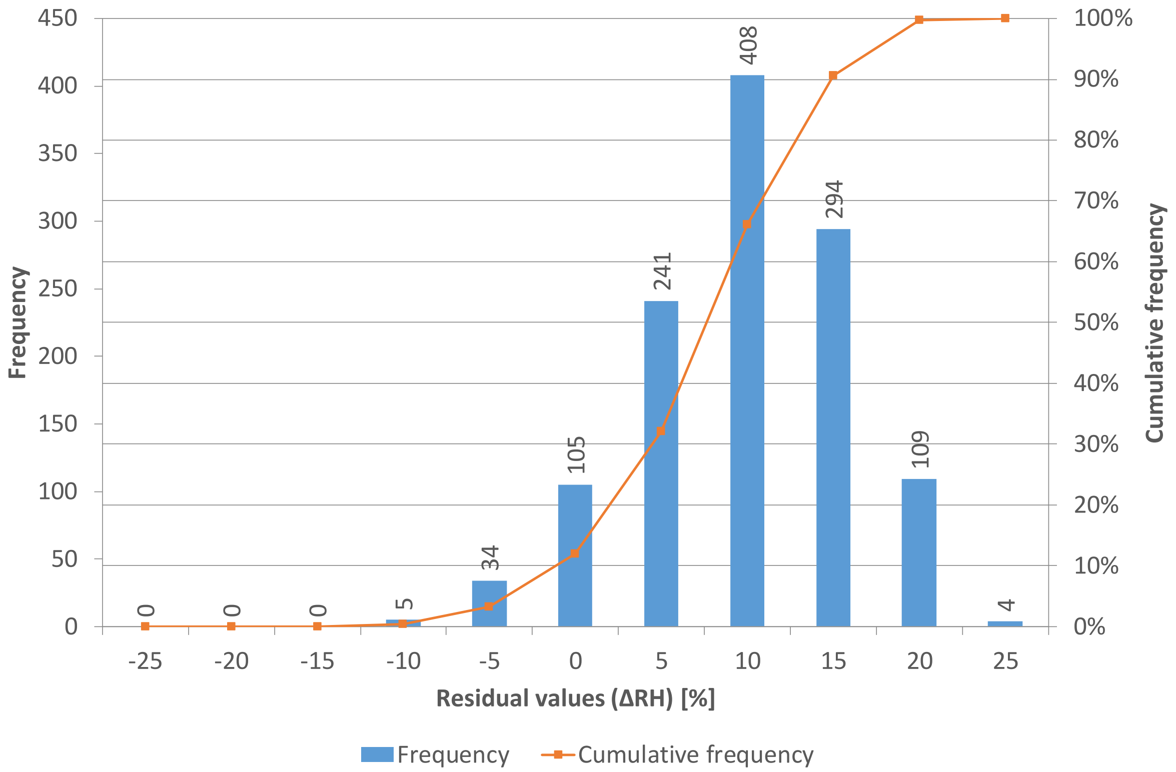

Fig. 14. Frequency and cumulative frequency of the residual values between the simulated values (S_i) and monitored values (M_i) concerning indoor air RH calculated on hourly basis (1200 values).

4.5 Reliability of the energy consumption estimation

The last part of the model validation concerns the energy consumption for heating (thermal energy) and ventilation (electrical energy).

The monitored working time of each gas heater of the house is reported in Table 8. The dataset shows that gas heaters I and V are the ones that were more activated each day, since they are located at the head and bottom of the house where the thermal losses due to transmission and infiltration are greater.

Knowing the working time and the heating capacity of each gas heater, the total energy consumption for space heating is calculated to be 3551 kWh. The energy consumption for space heating estimated by the model is 3184 kWh. These values indicate that the model slightly underestimates the thermal energy needed to heat the house of about 10%.

The monitoring campaign recorded 5061 kWh as electrical energy consumption of the ten fans for both base and tunnel ventilation. The presented model estimates that the electrical energy consumption is 5463 kWh, with a slight overestimation of 7.9%.

Table 8 – Monitored working time (in minutes) of the five gas heaters in the broiler house. Space heating results to be activated during the first 25 days of the batch.

Day of the batch	Gas heater monitored working time (minutes)				
	I	II	III	IV	V
1	365	125	8	9	386
2	712	264	8	7	600
3	612	307	12	9	566
4	574	315	3	6	571
5	506	256	3	0	525
6	435	224	0	3	441
7	370	212	0	0	407
8	290	285	0	0	369
9	181	232	0	0	274
10	169	208	0	0	179
11	415	496	27	239	452
12	444	408	8	2	509
13	201	229	4	1	321
14	160	189	5	30	246
15	128	197	0	0	52
16	145	187	14	197	181
17	190	251	0	0	210
18	422	401	34	355	93
19	380	393	66	653	48
20	132	155	8	1	3
21	95	100	3	40	25
22	56	81	1	328	155
23	25	14	0	45	0
24	11	6	0	0	1
25	6	4	2	0	0
26	0	0	0	0	0
27	0	0	0	0	0
28	0	0	0	0	0
29	0	0	0	0	0
30	0	0	0	0	0
Tot.	7024	5539	206	1925	6614

5 Conclusions

In the present work, the simulation model for the estimation of the energy consumption for climate control in broiler houses was presented. This model is based on a customization of the simple hourly method of ISO 13790 Standard. Solving the energy balance, the moisture balance and calculating the fan performance, the developed simulation model can estimate the thermal energy consumption due to heating and the electrical energy consumption due to ventilation (both for IAQ control and free cooling). Furthermore, the presented model provides the main indoor environmental parameters, specifically indoor air temperature and relative humidity. The validation and calibration of the developed model was possible through a dataset of real data from a monitoring campaign that concerned an entire batch carried out in a broiler house.

This model aims to be a useful tool for engineers that may use it to evaluate different design alternatives and retrofit measures from the point of view of the building envelope and the climate control systems. Farmers may also benefit from the use of this model because it can provide data (e.g. costs associated to energy and indoor environmental parameters) for improving the management of the animal farming.

The model has proven to be reliable from both the points of view of the environmental parameters and the energy consumption estimation. Room for improvement lies in the relative humidity prediction. Future developments of the model should take into account the properties of moisture storage of the enclosure and a fine-tuning of the evaporative pads modeling, considering the decay of the evaporative effectiveness due to both the inlet air speed variation and the degradation of the material as a consequence of usage.

The model was developed in an electronic spreadsheet environment but a further improvement could be a more user-friendly interface. Future plans include upgrading to consider more aspects such as, for example, the calculation of the thermal humidity velocity index (THVI), for estimating hourly the conditions of thermal stress of the birds.

Finally, due to the considerable differences that farming of various animal species presents, similar simulation models should be developed for the animal species mainly reared in developed countries (e.g. fattening pigs, dairy cows and laying hens). The final aim should be to increase the information about the use of energy in animal farming.

6 Acknowledgements

This work has been supported by financial funding of SIR (Scientific Independence of young Researchers) 2014 “EPAnHaus – Energy Performance of livestock houses” project, grant number RBSI141A3A, funded by MIUR (Italian Ministry of Education, Universities and Research).

7 Nomenclature

7.1 Symbols

A	area of all surfaces facing the building zone	[m^2]
B	*coefficient*	[-]
b	coefficient	[-]
C	building fabric effective heat capacity	[$J \cdot K^{-1}$]
c	specific heat capacity	[$J \cdot kg^{-1} \cdot K^{-1}$]
d	animal age	[days]
E	energy consumption	[kWh]
f	coefficient	[-]
g	coefficient	[-]
H	heat transfer coefficient	[$W \cdot K^{-1}$]
h	specific enthalpy	[$kJ \cdot kg^{-1}$]
h_{is}	surface heat transfer coefficient	[$W \cdot m^{-2} \cdot K^{-1}$]
k	coefficient	[-]
L	length of the building	[m]
n	animal number	[broilers]
$\dot{m}$	mass flow rate	[$kg \cdot s^{-1}$]
p	pressure	[Pa]
Q	energy need	[Wh]
R	sensible fraction of heat emission	[-]
S	coefficient	[-]
SPF	Specific Fan Performance	[$m^3 \cdot kWh^{-1}$]
t	temperature	[°C]
v	air velocity	[$m \cdot s^{-1}$]
$\dot{V}$	ventilation volume flow rate	[$m^3 \cdot h^{-1}$]
w	animal weight	[kg]
x	humidity ratio	[$kg_{vapor} \cdot kg_{air}^{-1}$]
Δt	temperature differential	[°C]
Φ	heat load, heat flux	[W]
ε	saturation effectiveness of cooling pad	[-]
η	gas heater efficiency	[-]

ρ	volumetric mass density	[$kg \cdot m^{-3}$]

7.2 Subscripts

a, air	air
avg	average
b	broiler
base, bs	base ventilation
C	cooling
db	dry bulb
e	external, outdoor
ec	evaporative cooling
el	electrical energy
eff	effective
f	flock
fan	fan
fen	fenestration
H	heating
i, int	internal, indoor
lat	latent heat
m	mass related
max	maximum
nd	need
op	opaque
sens	sensible heat
s	surface
set	set point temperature
sol	solar
sup	supply
th	thermal energy
tot	total
tr	transmission
tv	tunnel ventilation
v	vapor
ve	ventilation

w	animal-weight related
wb	wet bulb
τ	time step
0	0 $W \cdot m^{-2}$ heat load related
10	10 $W \cdot m^{-2}$ heat load related

8 References

[1] United Nations, Department of Economic and Social Affairs, Population Division, World Population Prospects: The 2008 Revision, Highlights, Working Paper No. ESA/P/WP.210. United Nation, New York, New York, 2009.

[2] FAO, World Livestock 2011. Livestock in food security. FAO, Rome, Italy, 2011.

[3] FAO (Global Perspective Studies Unit), World Agriculture towards 2030/2050. Interim report, FAO, Rome, Italy, 2006.

[4] P.K. Thornton and P. Gerber, Climate change and the growth of the livestock sector in developing countries, Mitigation and Adaptation Strategies for Global Change 15, 2010.

[5] L. Deutsch, M. Kalkenamrk, L. Gordon, J. Rockstrom, K. Folke, Water-mediated ecological consequences of intensification and expansion of livestock production, in H. Steinfeld, H. Mooney, F. Schneider, L. Neville (Eds.), Livestock in a changing landscape, Vol. 1: Drivers, consequences, and responses, Island Press, Washington DC, 2010.

[6] P.K. Thornton, Livestock production: recent trends, future prospects, Philosophical Transaction of the Royal Society 365, 2010.

[7] United Nations Framework Convention on Climate Change, Challenges and opportunities for mitigation in the agricultural sector: technical paper. United Nation Framework Convention on Climate Change, 2008.

[8] U. De Corato, F.A. Cancellara, L'efficienza energetica nel comparto zootecnico. Analisi dei consumi energetici e miglioramento delle performance di efficienza energetica in alcune tipologie di allevamento. ENEA, Roma, Italia, 2014.

[9] Rossi P, Gastaldo A, Riva G, de Carolis C., Progetto Re Sole (Final Draft), Centro Ricerche Produzioni Animali (CRPA), Reggio Emilia, Italy, 2013.

[10] A. Costantino, E. Fabrizio, A. Biglia, P. Cornale, L. Battaglini, Energy use for climate control of animal houses: the state of the art in Europe, Energy Procedia 101, 2016.

[11] ASHRAE, ASHRAE Handbook-HVAC Systems and Equipment, SI Edition, Atlanta, Georgia, 2008.

[12] European Commission, Joint Research Centre, Best Available Techniques (BAT) Reference Document for the Intensive Rearing of Poultry or Pigs (Final Draft). European Commission, Brussels, Belgium, 2015.

[13] FAOSTAT. Url: http://faostat3.fao.org/download/Q/QL/E (accessed on 14th November 2016).

[14] E. Fabrizio, G. Airoldi, R. Chiabrando, Study of the environmental control of sow farrowing rooms by means of dynamic simulation, Lecture Notes in Electr Eng, 263 (2014), 3-11.

[15] P. Axaopoulos, P. Panagakis, S. Kyritsis, Computer simulation assessment of the thermal mocroenvironment of growing pigs under summer conditions, Trans ASAE 35(1992) 1005-1009.

[16] J. Hamilton, M. Negnevitsky, X. Wang, Thermal analysis of a single-storey livestock barn, Advances in Mechanical Engineering 8 (2016) 1-9.

[17] P. Panagakis, P. Axaopoulos, Compare fogging strategies for pig rearing using simulations to determine apparent heat-stress indices, Biosystem Engeneering 99 (2008) 112-118.

[18] ISO 13790, Energy performance of buildings, Calculation of energy use for space heating and cooling, 2008.

[19] D. Marchio, J.R. Millet, O. Morisot, Simple modeling for energy consumption estimation in air conditioned buildings, Proceedings of Clima 2000, Brussel, Belgium (1997).
[20] S. Roujol, E. Fleury, D. Marchio, J.R. Millet, P. Stabat, Testing the energy simulation building model of Consoclim using Bestest method and experimental data, Proceedings of 8th IBPSA Conference (International Building Performance Simulation Association), Eindhoven, Netherlands (2003).
[21] P. Michalak, The simple hourly method of EN ISO 13790 standard in Matlab/Simulink: A comparative study for the climatic conditions of Poland, Energy 75 (2014) 568-578.
[22] M. Atmaca, E. Kalaycioglu, Z. Ylmaz, Evaluation of the heating & cooling energy demand of a case residential building by comparing the national calculation methodology of Turkey and EnergyPlus through thermal capacity calculations. Technical Report Energy Systems Laboratory, Texas A&M University, 2011.
[23] J.R. Millet, The simple hourly method of prEN 13790: a dynamic method for the future, Proceeding of Clima, Helsinki, Finland (2007).
[24] G. Kokogiannakis, J.A. Clarke, P.A. Strachan, The impact of using different models in practice - a case study with the simplified methods of EN ISO 13790 standard and detailed modeling programs, Proceedings of 10th IBPSA Conference (International Building Performance Simulation Association), Beijing, China (2007).
[25] G. Kokogiannakis, G.A. Strachan, J.A. Clarke, Comparison of the simplified methods of the ISO 13790 standard and detailed modelling programs in a regulatory context, Journal of Building Performance Simulation, 4 (2008) 209–219.
[26] A. Costantino, I. Ballarini, E. Fabrizio, Comparison between simplified and detailed methods for the calculation of heating and cooling energy needs of livestock housing: a case study, 3rd IBPSA-Italy Conference, 8th-10th February 2017, Bozen-Bolzano, Italy.
[27] X. Tao, H. Xin, Acute Synergistic effects of air temperature, humidity, and velocity on homeostasis of market-size broilers. Transaction of the ASAE (46), 2003.
[28] A. Gottfried, L’edilizia per l’agricoltura e la zootecnia, Editore Ulrico Hoepli, Milano, 2006.
[29] R. Chiumenti, Costruzioni rurali, Edagricole Scolastico, Milano, 2004.
[30] European Council, Directive 2007/43/C of European Council of 28th June 2007 on Laying down minimum rules for the protection of chickens kept for meat production.
[31] Arbor Acres, Broiler Management Guide, Aviagen, Huntsville, Alabama, 2007.
[32] Lohmann Meat, Broiler Stock Performance Objectives, Aviagen, Huntsville, Alabama, 2007.
[33] M.E. Esmay, J.E. Dixon, Environmental control for agricultural buildings, The AVI Publishing company, Inc., Westport, Connecticut, 1986.
[34] E.H. Bartali, A. Jongebreur, D. Moffitt, CIGR Handbook of Agricultural Engineering (Volume II), American Society of Agriculture Engineers, St Joseph, Michigan, 1999.
[35] D. R. Charles, Practical ventilation and temperature control for poultry, in: J. A. Clark (Eds.), Environmental aspects of housing for animal production, Page Bros, Norwich, United Kingdom, 1981.
[36] ASHRAE, ASHRAE Handbook-HVAC Applications, SI Edition, Atlanta, Georgia, 2007.
[37] S.B. Shah, J.L. Grimes, E.O. Oviedo-Rondón, P.W. Westerman, Acidifier application rate impacts on ammonia emissions from US roaster chicken house, Atmospheric Environment, Vol. 92 (2014), 576-583.
[38] M. Cambra-López, A.J.A. Aarnink, Y. Zhao, S. Calvet, A.G. Torres, Airborne particulate matter from livestock production systems: A review of an air pollution problem, Environmental Pollution 158 (2010), 1-17.
[39] J.P. Harner, J. Smith, Water consumption of an evaporative cooling system in the Midwest, Kansas Agricultural Experiment Station Research Reports, Vol. 0: Iss. 2 (2009).
[40] H. Han, K. Kim, K.-J. Jang, G.-S. Han, I.-B. Lee, Energy consumption and indoor environment of broiler houses with energy recovery ventilators, Applied Engineering in Agriculture, Vol. 29: Iss. 5 (2013).
[41] S.-W. Hong, I.-B. Lee, I.-H. Seo, K.-S. Kwon, The design and testing of a small-scale wind turbine fitted to the ventilation fan for a livestock building, Computers and Electronics in Agriculture, Vol. 99 (2013), 65-76.

[42] Y. Liang, G.T. Tabler, A.W. Reynolds, R. Starkweather, K.N. Jensen, Heat recovery ventilators in a broiler house to reduce energy use, American Society of Agricultural and Biological Engineers (ASABE) Annual International Meeting, 7th-10th August 2011, Louisville, Kentucky, USA.
[43] P.A. Pereira, T.Jr. Yanagi, J.P. Da Silva, R.R. Lima, A.T. Campos, L.H.P. Abreu, Lighting systems for broiler houses, American Society of Agricultural and Biological Engineers (ASABE) Annual International Meeting, 29th July – 1st August 2012, Dallas, Texas, USA.
[44] P.A.P. Ribeiro, T.Jr. Yanagi, J.P. Da Silva, S.D.N.M. Yanagi, R.S. Campos, Technical-economic analysis of different lighting systems for broiler poultry, Engenharia Agricola, Vol. 36: Iss. 2 (2016), 242-252.
[45] M. Rajaniemi, J. Ahokas, Direct energy consumption and CO_2 emissions in a Finnish broiler house – A case study, Agricultural and Food Science, Vol.24: Iss. 1 (2015), 10-23.
[46] M. Rajanimei , J. Tuure, J. Ahokas, Heating energy consumption, heat losses and heating energy saving possibilities in case broiler house in Finland, American Society of Agricultural and Biological Engineers (ASABE) Annual International Meeting, 21th 24th July 2013, Kansas City, Missouri, USA.
[47] M. Rajaniemi, J. Ahokas, A case study of energy consumption measurement system in broiler production, Agronomy Research, Vol. 10: Iss. SPEC. ISS. 1 (2012), 195-204.
[48] Y. Liang, G.T. Tabler, S.E. Watkins, H. Xin, I.L. Berry, Energy use analysis of open-curtain vs. totally enclosed broiler houses in Northwest Arkansas, Applied Engineering in Agriculture, Vol. 25: Iss. 4 (2009), 577-584.
[49] T. Kalhor, A. Rajabipour, A. Akram, M. Sharifi, Modeling of energy ratio index in broiler production units using artificial neural networks, Sustainable Energy Technologies and Assessments 17 (2016), 50-55.
[50] M.M. Vale, D.J. Moura, I.A. Nääs, D.F. Pereira, Characterization of heat waves affecting mortality rates of broilers between 29 days and market age, Revista Brasileira de Ciencia Avicola, Vol.12: Iss. 4 (2010), 279-285.
[51] L. Galiot, I. Lachance, J. Laforest, F. Guay, Modelling piglet growth and mortality on commercial hog farms using variables describing individual animals, litters, sows and management factors, Animal Reproduction Science (In press).
[52] P.F.P. Ferraz, T.Y. Junior, Y.F.H. Julio, J. de Oliveira Castro, R.S. Gates, G.M. Reis, A.T. Campos, Predicting chick body mass by artificial intelligence-based models, Pesquisa Agropecuaria Brasileira, Vol. 49: Iss. 7 (2014), 559-568.
[53] C.A. Rotz, Modeling greenhouse gas emissions from dairy farms, Journal of Dairy Science 101, 1-16 (In press).
[54] J. Dekock, E. Vranken, E. Gallman, E. Hartung, D. Berckmans, Optimisation and validation of the intermittent measurement method to determine ammonia emissions from livestock buildings, Biosystems Engineering 104 (2009), 396-403.
[55] J. Hendriks, A. Andries, P. Saevels, C. Leribaux, E. Vranken, C. Vinkier, D. Berckmans, Development of a simplified procedure for determination of odor and ammonia emissions of agricultural buildings on behalf of environmental legislation in Flanders, Internal Report PBO Study of the Flemish Government, 2001.
[56] B. Bjerg, G. Cascone, I.B. Lee, T. Bartzanas, T. Norton, S.W. Hong, I.H. Seo, T. Banhazi, P. Liberati, A. Marucci, G. Zhang, Modelling of ammonia emissions from naturally ventilated livestock buildings. Part 3: CFD modelling, Biosystem Engineering 116 (2013), 259-275.
[57] E. Bustamante, S. Calvet, F. Estellés, A.G. Torres, A. Hospitaler, Measurement and numerical simulation of single-sided mechanical ventilation in broiler houses, Biosystems Engineering 160 (2017), 55-68.
[58] D. Fidaros, C. Baxevanou, T. Bartzanas, C. Kittas, Numerical study of mechanically ventilated broiler house equipped with evaporative pads, Computers and Electronics in Agriculture (In press).
[59] F. Rojano, P.E. Bournet, M. Hassouna, P. Robin, M. Kacira, C.Y. Choi, Modelling heat and mass transfer of a broiler house using computational fluid dyanmics, Biosystems Engineering 136 (2015), 25-38.

[60] F. Rojano, P.E. Bournet, M. Hassouna, P. Robin, M. Kacira, C.Y. Choi, Computational modelling of thermal and humidity gradients for a naturally ventilated poultry house, Biosystems Engineering 151 (2016), 273-285.
[61] K. Kwon, I. Lee, G.Q. Zhang, T. Ha, Computational fluid dyanmics analysis of the thermal distribution of animal occupied zones using the jet-drop-distance concept in a mechanically ventilated broiler house, Biosystems Engineering 136 (2015), 51-68.
[62] I. Seo, I. Lee, O. Moon, S. Hong, H. Hwang, J.P. Bitog, K. Kwon, Z. Ye, J. Lee, Modelling of internal environmental conditions in a full-scale commercial pig house animal, Biosystems Engineering 111 (2012) 91-106.
[63] H. Li, L. Rong, C. Zong, G. Zhang, A numerical study on forced convective heat transfer of a chicken (model) in horizontal airflow, Biosystems Engineering 150 (2016), 151-159.
[64] ASABE (American Society of Agricultural and Biological Engineers), ASAE EP270.5 DEC1986 (R2012) – Design of Ventilation Systems for Poultry and Livestock Shelters.
[65] ASABE (American Society of Agricultural and Biological Engineers), ANSI/ASASE EP282.2 FEB1993 (R2013) – Design Values for Emergency Ventilation and Care of Livestock and Poultry.
[66] ASABE (American Society of Agricultural and Biological Engineers), ASAE EP344.4 JAN2014 – Lighting Systems for Agricultural Facilities.
[67] ASABE (American Society of Agricultural and Biological Engineers), ASAE EP294.3 SEP2003 (R2013) – Computing Electrical Demands for Farms.
[68] ASABE (American Society of Agricultural and Biological Engineers), ANSI/ASABE S612 JUL2009 – Performing On-farm Energy Audits.
[69] M.A. Hellickson, J.N. Walker, Ventilation of agricultural structures, ASAE Monograph Number 6, American Society of Agricultural Engineers, St. Joseph, Michigan, 1983.
[70] Lohmann Meat, Broiler Stock Performance Objectives, Aviagen, Huntsville, Alabama, 2007.
[71] Cobb, Broiler Management Guide, Cobb, Siloam Springs, Arkansas, 2008.
[72] T.M.R. De Carvalho, D.J. De Moura, P.A.M. Leal, J.M. Massari, K.A.O. Lima, Heat transfer to calculate minimum ventilation rates for broiler house, American Society of Agricultural and Biological Engineers (ASABE) – 9th Interantional Livestock Environment Symposium (ILES), 8th – 12th July 2012, Valencia, Spain.
[73] ISO 13786, Thermal performance of building components – Dynamic thermal characteristics – Calculation methods, 2007.
[74] E. Fabrizio, V. Monetti, Methodologies and Advancements in the Calibration of Building Energy Models, Energies 8 (2015) 2548-2574.
[75] M. Royapoor, T. Roskilly, Building model calibration using energy and environmental data, Energy and Buildings, 94 (2015) 109-120.
[76] G. Mustafaraj, D. Marini, A. Costa, M. Keane, Model calibration for building energy efficiency simulation, Applied Energy 130 (2014) 72-85.
[77] A. Cacabelos, P. Eguía, L. Fabrero, E. Granada, Development of a new multi-stage building energy model calibration methodology and validation in a public library, Energy and Buildings 146 (2017) 182-199.
[78] ASHRAE (American Society of Heating, Refrigerating and Air-Conditioning Engineers), ASHRAE Guideline 14-2002: Measurement of Energy Demand and Savings, Atlanta, Georgia, 2002.